MICROCOPY RESOLUTION TEST CHART
NATIONAL BUREAU OF STANDARDS-1963-A

LEVEL

ADA064761

CATHODOLUMINESCENCE ON THE
EFFECTS OF Te IMPLANTATION
AND LASER ANNEALING IN
GALLIUM ARSENIDE

THESIS

AFIT/GEP/PH/78D-8   Ronald L. Lusk
                          Captain   USAF

DDC

FEB 22 1979

A

79 01 30 167

CATHODOLUMINESCENCE ON THE

EFFECTS OF Te IMPLANTATION AND

LASER ANNEALING IN GALLIUM ARSENIDE.

Master's thesis,

THESIS

65 P.

2306

R2

Presented to the Faculty of the School of Engineering

of the Air Force Institute of Technology

Air Training Command

In Partial Fulfillment of the

Requirements for the Degree of

Master of Science

by

Ronald L. Lusk

Captain   USAF

Graduate Engineering Physics

December 1978

012 225

Preface

The completion of this thesis would not have been possible without the advice and assistance of other people. First, I would like to express my thanks to my faculty advisors, Dr. Robert L. Hengehold and Dr. Theodore E. Luke. They offered many useful suggestions and were always approachable for discussion. Next, I would like to thank 2Lt. Jamie G. Varni with whom I had many discussions which clarified the material. I would also like to express my gratitude for the fine technical assistance and advice given to me by Jim Miskimen, George Gergal, and Ron Gabriel of the AFIT Physics Laboratory staff. Finally, I would like to thank my wife for her understanding during the time I was absorbed in study and for the help she provided in writing this thesis.

Contents

List of Figures

List of Tables

Abstract

Six Te implanted GaAs samples were examined by the method of cathodoluminescence to determine the effect of laser annealing. Two of the samples (one 10^{13} fluence and one 10^{14} fluence) were thermally annealed, one sample (10^{13} fluence) was unannealed, and three samples (10^{13} fluence) were laser annealed.

When a laser energy density of 0.07 J/cm^2 was used, it was found that only a small percentage of the Te ions moved to substitutional sites and the laser radiation created Ga vacancies.

When a laser energy density of 0.6 or 0.8 J/cm^2 was used, the implant layer was damaged by the laser radiation and all luminescence from the implant layer was quenched. Further, the luminescence that was detectable (only at the maximum beam energy of 15KV) was characteristic of the substrate, not the implanted layer.

CATHODOLUMINESCENCE ON THE EFFECTS

OF Te IMPLANTATION AND LASER

ANNEALING IN GALLIUM ARSENIDE

I. Introduction

The United States Air Force uses devices which must operate in

high temperature environments where intrinsic (pure) semiconductors

do not perform well. With the intentional addition of impurity ions

(doping) into the lattice of a crystal, the semiconductor gallium arse-

nide (GaAs) should have the electrical properties required for opera-

tion in the environments mentioned above.

Gallium arsenide is an intermetallic compound formed from a group

III element (gallium) and a group V element (arsenic). It crystallizes

in the zinc blende structure and has physical properties which are sim-

ilar to those of the covalent group IV semiconductors, germanium and

silicon. The electrical properties, such as high electron mobility,

have made GaAs very useful in many technical applications. However,

the promise that GaAs shows for use in future devices, such as micro-

wave devices, is based upon the ability to provide the necessary im-

purity concentrations in the 'pure' crystal.

The Air Force Avionics Laboratory (AFAL), Wright-Patterson Air

Force Base, Ohio, is currently ion implanting GaAs with Tellurium (Te).

The ion implantation process requires that impurity atoms be ionized,

accelerated to high energies, and allowed to bombard the target crystal.

After striking the crystal, the energetic ions are gradually

1

slowed by collisions with crystal atoms. During these collisions, energy is transferred to the crystal atoms, and, if the transferred energy is great enough, the atoms are displaced from their normal lattice sites and damage is produced within the crystal.

Before useful electrical activity can be obtained, this damage must be removed by annealing (heat treating) the crystal. During thermal annealing, the crystal is heated to high temperatures for long periods of time, and the impurity atoms move to lattice sites. However, one problem with this method is that not only do the impurity atoms move, but Ga and As atoms also move and vacancies are created. In an attempt to anneal crystals and avoid the high temperature problems, laser annealing is being studied. A Q-switched laser provides the ability to heat the crystal for a very short period of time.

The purpose of this study is to examine the damage created by Te implantation, to determine the affects of laser annealing on this damage, and to investigate the lattice structure with respect to Te ion positions and the presence of native defects. The experimental technique of cathodoluminescence is used to study the luminescence from various depths within the samples. This technique had been used to study GaAs (Ref 14) and ZnO (Ref 34). Luminescence is a phenomenon in which electron-hole pairs recombine and release energy in the form of visible or infrared radiation. There are several common ways to excite a crystal and produce luminescence: by the use of photons (photoluminescence), thermally (thermoluminescence), electrically (electroluminescence), and by the use of a beam of energetic electrons (cathodoluminescence). The advantage of cathodoluminescence is that it is possible to investigate the luminescence from different depths in the crystal by varying the beam voltage and thus the energy of the electrons.

Chapter II of this report contains the theory necessary to support arguments presented in later chapters. Chapter III contains a description of the experimental apparatus and procedures used. Chapter IV discusses the experimental results, and Chapter V presents some conclusions and recommendations.

II. Theory

This chapter contains the background theory necessary for an adequate understanding of the results discussed in Chapter IV. The theory is discussed in six sections; Luminescence, Cathodoluminescence from Gallium Arsenide, Impurity Concentration Dependence on Luminescence, Ion Implantation, Annealing, and Electron Beam Penetration in Gallium Arsenide.

Luminescence

Luminescence, as stated in Chapter I, is the radiation emitted by the recombination of electron-hole pairs. There are several different radiative recombinations possible. The simple energy band diagram in Figure 1 will be used to illustrate four different kinds: free-free, exciton, free-bound, and bound-bound. In this diagram, the conduction band represents a continuum of excited energy states to which electrons can be raised from their normal ground state. Their ground state is represented by the valence band, and the energy gap between the valence and conduction bands is the region where energy levels are normally forbidden. Energy levels in the band-gap are caused by excitons, impurity atoms, or lattice imperfections.

The first transition in Figure 1 is the recombination of a free electron (e) in the conduction band with a free hole (h) in the valence band. The energy of this transition is equal to the band-gap energy (E_G).

The second transition shown in Figure 1 represents the recombination of an exciton. An exciton is an electron bound to a hole in a manner similar to an electron in the hydrogen atom. An exciton

4
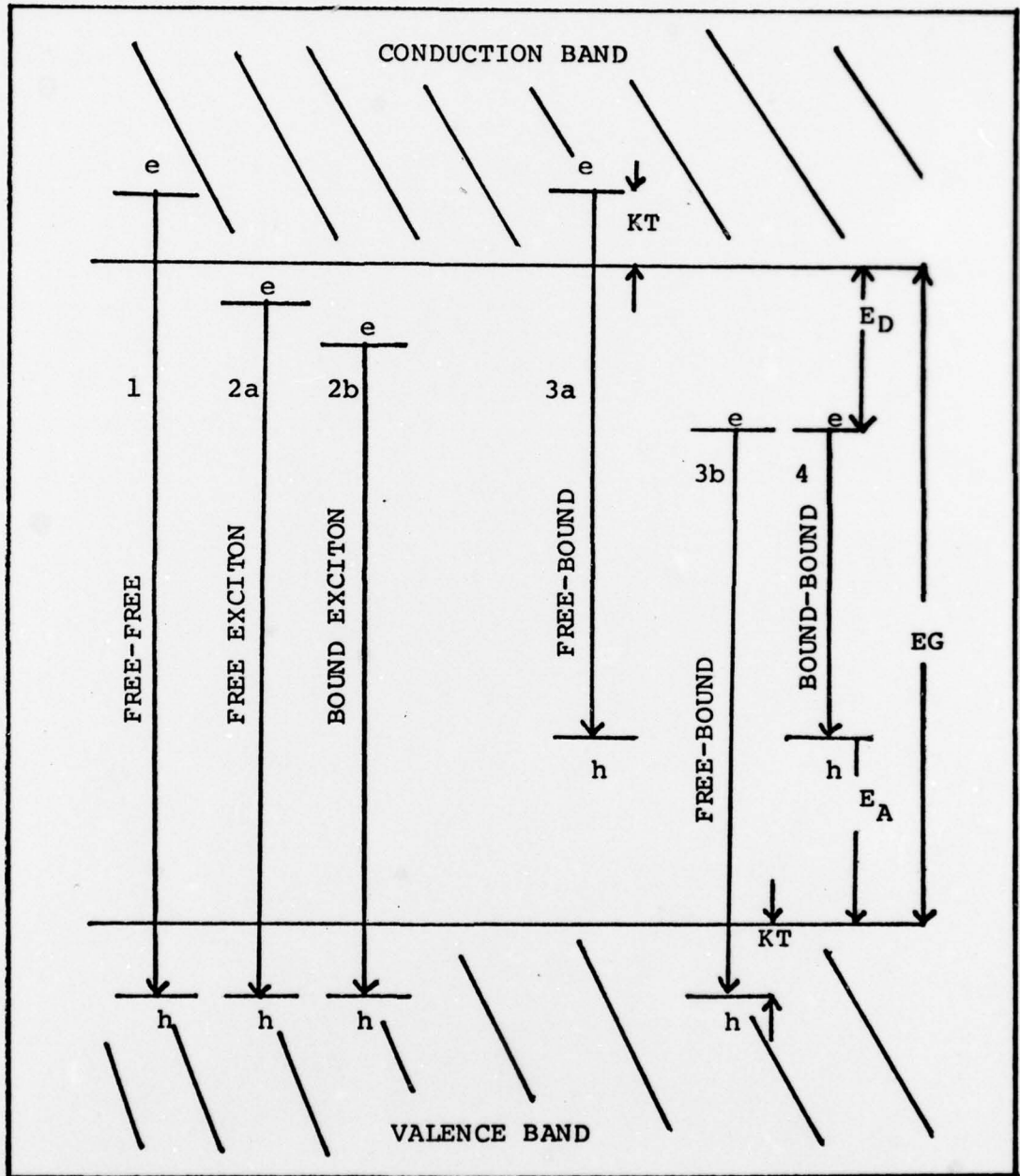
Figure 1. Simple Energy Band Diagram

5

can be either free or bound to a lattice site. The energy of the free exciton is less than the bandgap by an amount approximately equal to the coulombic force between the electron and hole (Ref 25: 332). The energy emitted by a bound exciton (transition 2b) is less than that of a free exciton by the amount necessary to bind the exciton to an impurity site (Ref 3:6).

Free-bound transitions are the third transition depicted in Figure 1. Transition (3a) represents the recombination of a free electron with a hole bound to an acceptor impurity, and transition (3b) represents the recombination of an electron bound to a donor impurity with a free hole. The energy of this transition is given by (Ref 8:744):

$$E = E_G - E_B + KT \pm nE_p \tag{1}$$

where

E = energy of the emitted photon

E_G = band-gap energy

E_B = binding energy of the electron (E_D) or the hole (E_A)

K = Boltzmann's constant

T = absolute temperature

n = number of photons

E_p = optical phonon energy

The last term in Eq (1) represents discrete amount of energy which can be given up to or absorbed from the crystal lattice in the form of lattice vibrations. These quanta of energy are called phonons (Ref 25:117). The third term in Eq (1) represents the thermal energy of

6

the free electron or free hole. This term is sometimes taken to be 3 KT/2 or KT/2 (Ref 1:1051, 10:151). With respect to the band-gap energy, this term will cause the energy of the emitted photon to decrease as crystal temperature decreases. The band-gap energy, however, increases as temperature decreases (Ref 35:770).

The final transition depicted in Figure 1 is the recombination of an electron bound to a donor impurity and a hole bound to an acceptor impurity. If the distance between the donor and acceptor impurities is much greater than the Bohr radii of the bound electron and hole, the energy of the bound-bound transition can be approximated by (Ref 13:789, 31:4):

$$E = E_G - (E_A + E_D) + e^2/kR \tag{2}$$

where

E = energy of emitted photon

E_G = band-gap energy

E_A = acceptor binding energy

E_D = donor binding energy

e = electronic charge

k = dielectric constant of the host crystal

R = separation distance between donor and acceptor

The last term in Eq (2) accounts for the coulomb interaction between the hole and electron. Since R is a discrete number corresponding to the spacing between the various donor-acceptor pairs in the crystal lattice, one expects to observe a series of sharp spectral lines. However, in many cases, these discrete donor-acceptor lines are not resolvable and appear as a broad peak which is the envelope of several unresolved lines (Ref 13:789). Like the band=gap energy, this

term is also a function of temperature. As the temperature increases, carriers are thermally released from donor sites and move to more favorable positions for recombinations, positions for which R is smaller (Ref 13:792, 14:5). This causes the energy of the peak to shift towards higher energy which offsets the opposite shift caused by the band-gap energy. Therefore, as the temperature increases, the energy of the bound-bound peak shifts toward lower energy by a smaller amount than the band-gap shift. Another way to identify bound-bound transitions (other than observing the peak shift with temperature) is to observe the peak shift vs excitation intensity. It is a well established fact that close pairs decay more rapidly than distant pairs. Increasing the excitation intensity will favor the closer pairs and, according to Eq (2), the peak will move toward higher energies (Ref 13:791, 38:335-6).

Cathodoluminescence from Gallium Arsenide

The radiative recombination from GaAs can be grouped into two categories according to the type of center that is responsible for the transition. These two categories are simple centers and complex centers.

Simple Centers. A simple center is defined by Willardson and Beer (Ref 38) as an impurity which sits on a gallium or arsenic lattice site and contributes one additional carrier (electron or hole) to the binding. The radiative recombinations described in the previous section are all due to simple centers. The optical activation energy for a single carrier bound to an impurity is close to that calculated from a hydrogenic model. For a donor this energy is approximately 5-6 meV and for an acceptor approximately 20-42 meV (Ref 38:328-329).

8

The radiative recombinations from simple centers in GaAs have energies which are close to the band-gap energy. At a temperature of $20^{\circ}K$, the band-gap energy is approximately 1.521eV, as are also the exciton transitions and the transitions from a donor to the valence band. The conduction band to acceptor transitions and the bound to bound transitions occur at approximately 1.49eV. The relative intensity and shape of the peaks from these recombinations are dependent upon impurity concentration, and it is often very difficult to identify which type is being observed (Ref 2, 10, 11, 13, 38:327-351, 41).

Complex Centers. A complex center is defined as a radiative center that produces an emission peak too broad and too low in energy to be a hydrogenic (simple) center (Ref 38:359). Several transitions from complex centers have been identified and are listed in Table I. Although a large number of studies have been completed, little is known about some of these deep level transitions. For example, there are two current theories for the 1.2eV peak. Some believe that this peak is the result of a gallium vacancy-donor complex and some believe that with Te-doped GaAs, the peak is the result of the formation of a solid solution of Ga_2Te_3. The temperature shift of the peaks from complex centers is opposite to that of the band-gap and is about half as great for the arsenic vacancy complexes as for the gallium vacancy complexes (Ref 19, 38:259-382).

Impurity Concentration Dependence on Luminescence

It has been shown that as the concentration of impurities increases a shift occurs in the luminescence peak energy of simple

9

Table I

Radiative Recombinations from Complex Centers

Peak Energy (eV)	Ref	Center Involved
1.40-1.47	4, 5, 6, 21	As Vacancy
1.37	4. 7	Ga Vacancy-Cu
1.36-1.37	3, 19	As Vacancy-Acceptor
1.23-1.36	6, 7, 19, 21	Ga Vacancy-Donor
1.20	7, 28, 30, 39, 40	Ga Vacancy-Te Donor
	26, 36, 38	Solid Solition of Ga_2Te_3
1.02	4	Ga Vacancy-As Vacancy
0.81	4	Ga Vacancy
0.70	4	As Vacancy
0.58	4	Ga Vacancy

centers for both n- and p-type GaAs. In both cases, this shift is due to the overlapping of the impurity wave functions which causes a broadening of the impurity level within the band-gap into a band. For n-type GaAs, banding begins with about a 5×10^{16} cm^{-3} concentration of carriers and the band merges with the conduction band at about 1×10^{17} cm^{-3}. For acceptors, banding starts at about 5×10^{17} cm^{-3} and the band merges with valence band at about 3×10^{18} cm^{-3} (Ref 10, 11, 37:325-327).

Figure 2 shows data taken from Cusano (Ref 10, 11) showing
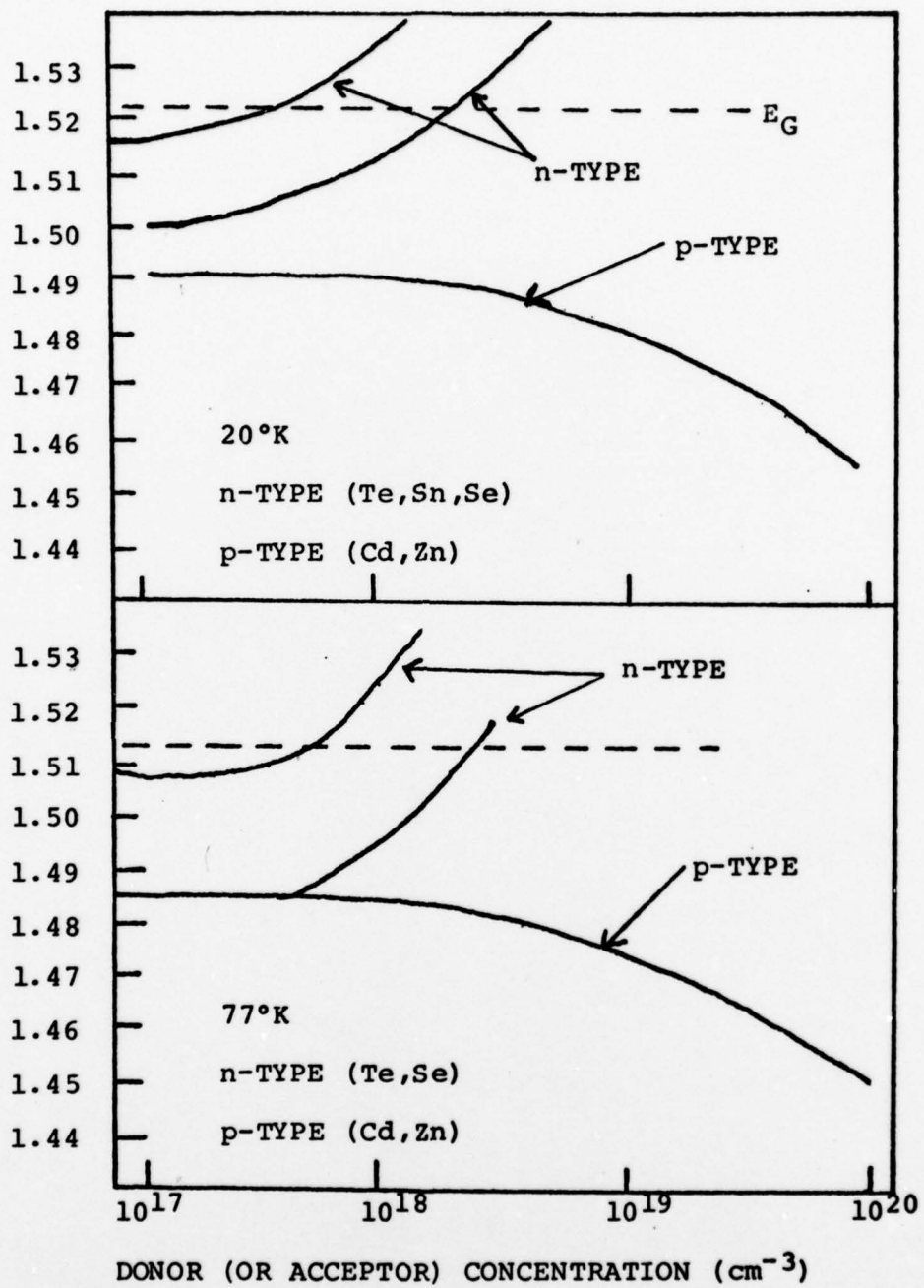
Figure 2. Peak Position vs Majority Dopant
(Ref 3, 10, 11)

11

emission peak shift as a function of dopant concentration. At either
temperature, the top curve shows the peak of a donor-valence band
recombination as it shifts into a free-free transition with increasing
donor doping. The middle curves trace the peak shift of a conduction
band-acceptor transition as the donor doping is increased. The bottom
curves show the peak shift of a conduction band-acceptor or donor-
acceptor transition with increasing acceptor doping.

Ion Implantation

Ion implantation is one method of introducing impurities into a
substrate. The process consists of ionizing the impurity atoms,
accelerating the ionized atoms through a high potential field, and
directing the beam of ions to bombard a substrate. Although some
of the impurity ions will be reflected, the majority will penetrate
the crystal. In this way, impurities can be introduced into a sub-
strate in concentrations, and in geometric patterns as desired while
simultaneously avoiding the high temperature problems of the diffusion
method of impurity doping (Ref 3, 15, 33).

After penetrating the surface of the crystal, the energetic ions
are gradually slowed by a series of collisions with the target nuclei
and electrons. Although the incident ions have nearly equal energy,
their penetration depths will vary due to the fact that both the num-
ber of collisions and the energy transferred per collision are random.
The distribution of ion stopping points can be predicted by using
the theory of Lindhard, Schoitt, and Scharff (LSS). In the LSS
theory, the impurity distribution is described by a gaussian func-
tion (Ref 27:3-5). Using this theory, the expected distribution of

12

Te prior to annealing was calculated using a mean projected range of 0.0328 microns (Ref 16) and is presented in Figure 3.

Annealing

The collisions described in the previous section not only slow the incident ions but create damage within the crystal. Damage is produced, first, by sputtering surface ions from the crystal, and second, by removing atoms from their lattice sites creating vacancies and interstitials. The second type of damage is more important as the crystalline structure is destroyed. These defects in the crystal-line structure must be removed before useful electrical activity can be attained. These defects can be removed by annealing the ion-implanted sample. Annealing not only recrystalizes the sample, but helps the impurity atoms to move to substitutional sites. There were two methods of annealing used in this study: thermal annealing and laser annealing.

Thermal Annealing. Thermal annealing is the process of heating the ion-implanted samples to high temperatures in an oven for long periods of time (sometimes as much as 24 hours) (Ref 4:143). It has been shown that in order for annealing to be effective on ion-implanted GaAs, temperatures in the range of $800^{\circ}C$ to $900^{\circ}C$ are necessary (Ref 5:568, 14:9, 18:601). However, at temperatures near $600^{\circ}C$, the GaAs surface begins to decompose. Si_3N_4 or SiO_2 caps have been success-fully used to protect the surface of the crystal to help prevent out diffusion of Ga and As which, if allowed, produces unwanted vacancies in the lattice structure (Ref 14:9). In addition to causing the out diffusion of Ga and As, annealing causes the implanted ions to diffuse

13
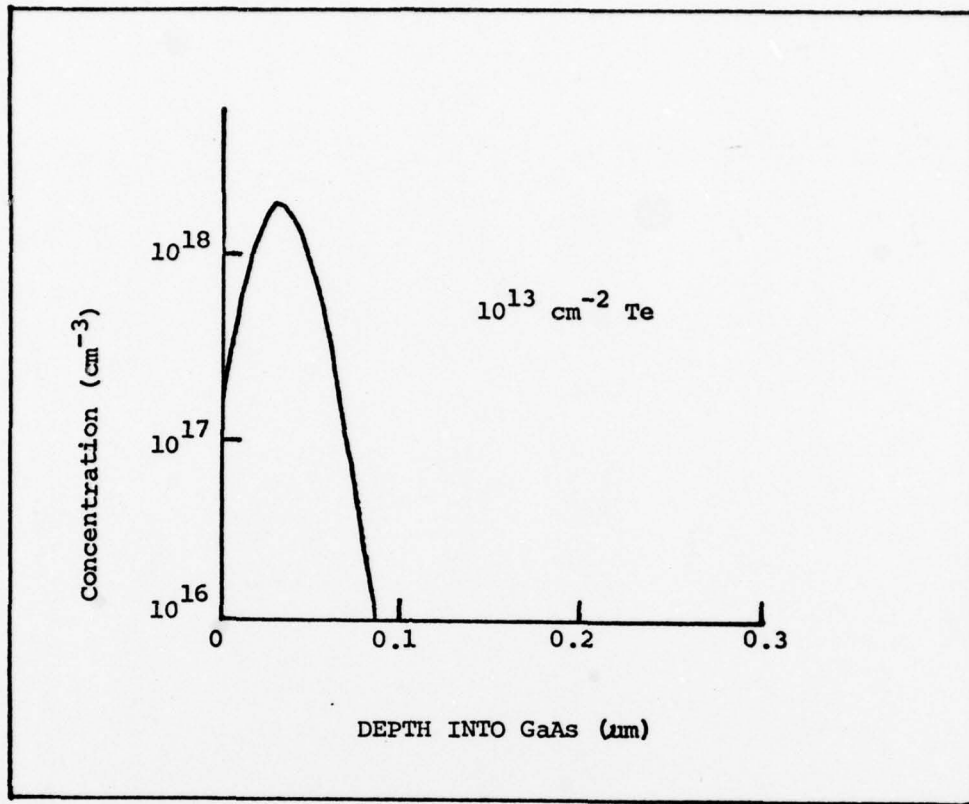
Figure 3. Projected Concentration Profile
for 120 KeV Te Implant

further into the GaAs crystal. This diffusion has been substantiated
by many experiments and is discussed in detail by Dumoulin (Ref 14:10-
12). In some applications this diffusion of the implanted ions may
be undesirable and it is thought that excessive diffusion can be avoided
by using a laser to anneal the samples.

Laser Annealing. Laser annealing consists of irradiating the
ion-implanted sample with a single short pulse of intense laser radi-
ation (Ref 17). A short pulse of light with photon energies exceeding
the band-gap energy will heat a thin surface layer of the sample. This
makes it possible to anneal the defects of the ion-implanted layers
without the undesirable heating of the bulk material (Ref 22, 24).

It has been found that a single laser pulse with a power density exceeding the threshold power is sufficient for crystallization of the amorphous layers and for electrical activation of the impurity atoms (Ref 22, 23). This threshold power for GaAs is 2×10^6 W/cm^2 (Ref 22). It has also been found that a single pulse is sufficient to anneal Te-doped GaAs.

Kachurin (Ref 23) has calculated that with laser annealing, the surface temperature of the sample does not rise by more than 150°C, and Golovchenko (Ref 17) observed that there was no significant decomposition of GaAs with laser annealing. These two facts make it possible to anneal GaAs without the use of a cap to protect the surface or prevent out diffusion of Ga or As. This low annealing temperature applied for a very short time may also decrease the diffusion of impurity atoms into the crystal.

Although laser annealing of ion-implanted silicon has been reported by several groups in the Soviet Union and a few studies have been made on the effect of laser annealing on GaAs, much is still unknown. The results so far have not been completely consistent nor understood. It is generally believed that heating is the main effect of laser pulses; however, studies need to be made to determine the effect of ionization, shock waves, the latent heat of crystallization, and the migration of impurities (Ref 22, 24).

Electron Beam Penetration in Gallium Arsenide

As a source of excitation, a beam of energetic electrons offers the advantage of being able to produce electron-hole pairs at various depths within the crystal. The depth to which electrons penetrate

15

when incident normally on GaAs has been measured. Although the total penetration depths are useful, the profile or distribution of penetration depths is also desired. Further, the penetration curves for electrons incident at 45° are required as the samples are oriented at a 45° angle to the electron beam. Norris et al (Ref 29) have used a method of scaling these curves by using the density of the crystal to be studied. Since these first estimates were made, new calculation methods have improved the accuracy of these profiles. Cone (Ref 9) has used standard Monte Carlo procedures to calculate the electron penetration profiles. This data is presented in Figure 4.
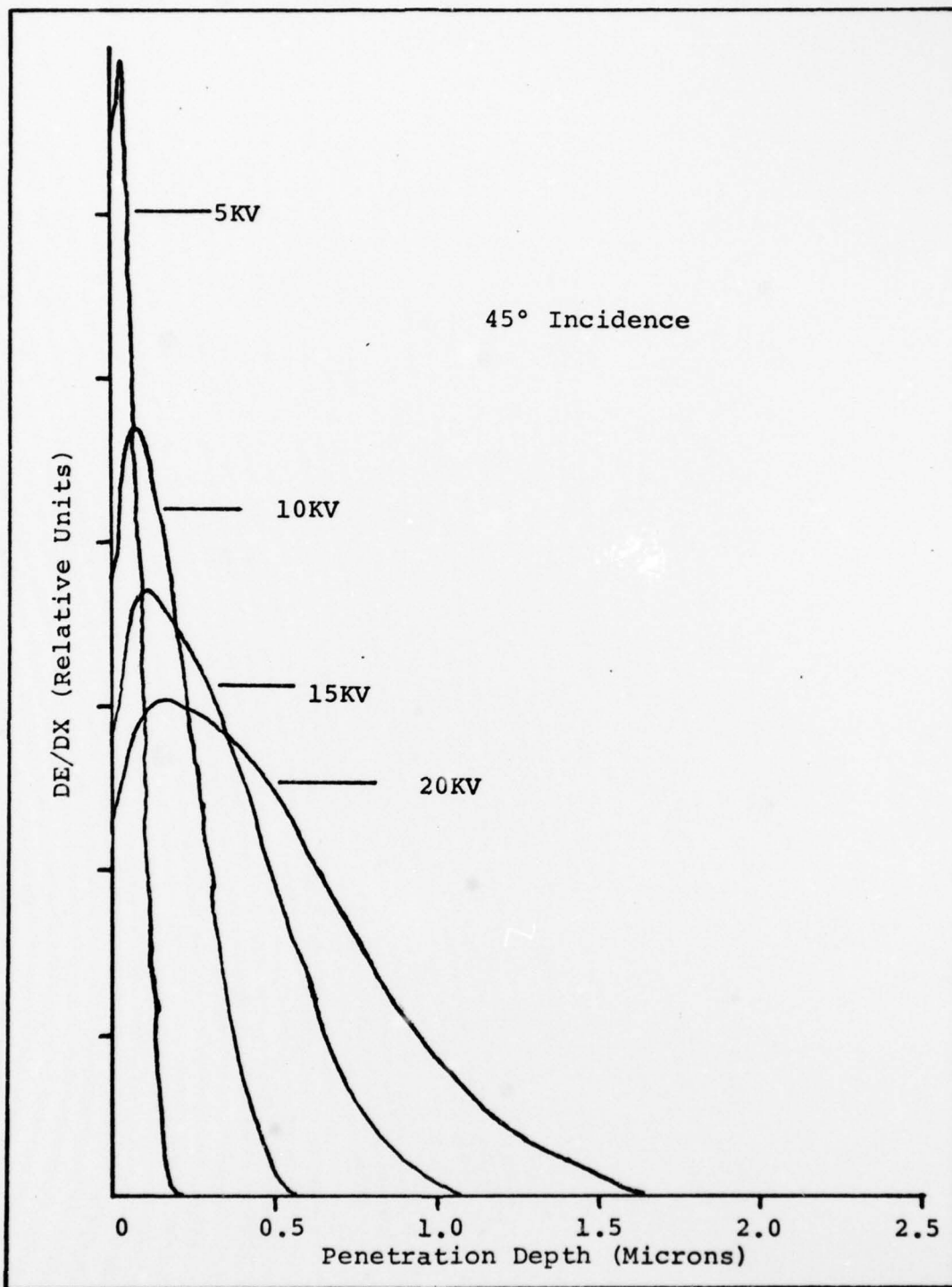
Figure 4. Electron Excitation Profiles

III. Experiment

The cathodoluminescence system in this experiment was similar to the system used by Daniels, and his thesis should be referenced by those who wish additional information on the apparatus (Ref 12:14-29). In order to study the effects of laser annealing on Te-implanted GaAs, it was necessary to use electron beam energies (E_B) in the range of 1-25KV with beam currents (I_B) between 1 and 7.5 microamperes. The cathodoluminescence system and the procedures used are described in this chapter.

Cathodoluminescence System

The cathodoluminescence system used in this experiment is shown schematically in Figure 5. A beam of energetic electrons from a vertically mounted electron gun struck a sample mounted on the cold finger of a liquid helium dewar. The cathodoluminescence from the sample passed through a quartz window of the sample chamber and was focused on the entrance slit of a 3/4 meter spectrometer by two lenses. The signal was detected by a cooled S1 photomultiplier mounted on the exit slit of the spectrometer. The electrical pulses from the photomultiplier were amplified by a wideband amplifier-discriminator unit, and the output from this unit was used to trigger a pulse generator. Finally, the pulses were counted by a multi-channel analyzer. This apparatus will be described in greater detail in four sections: Sample Environment, Excitation Source, Detection System, and Signal Recording System.

Sample Environment. The sample and electron gun chambers were maintained at a vacuum of approximately 2×10^{-7} torr with liquid nitrogen

18

Figure 5. Cathodoluminescence System Schematic

as the coolant and approximately 1×10^{-8} torr with liquid helium.
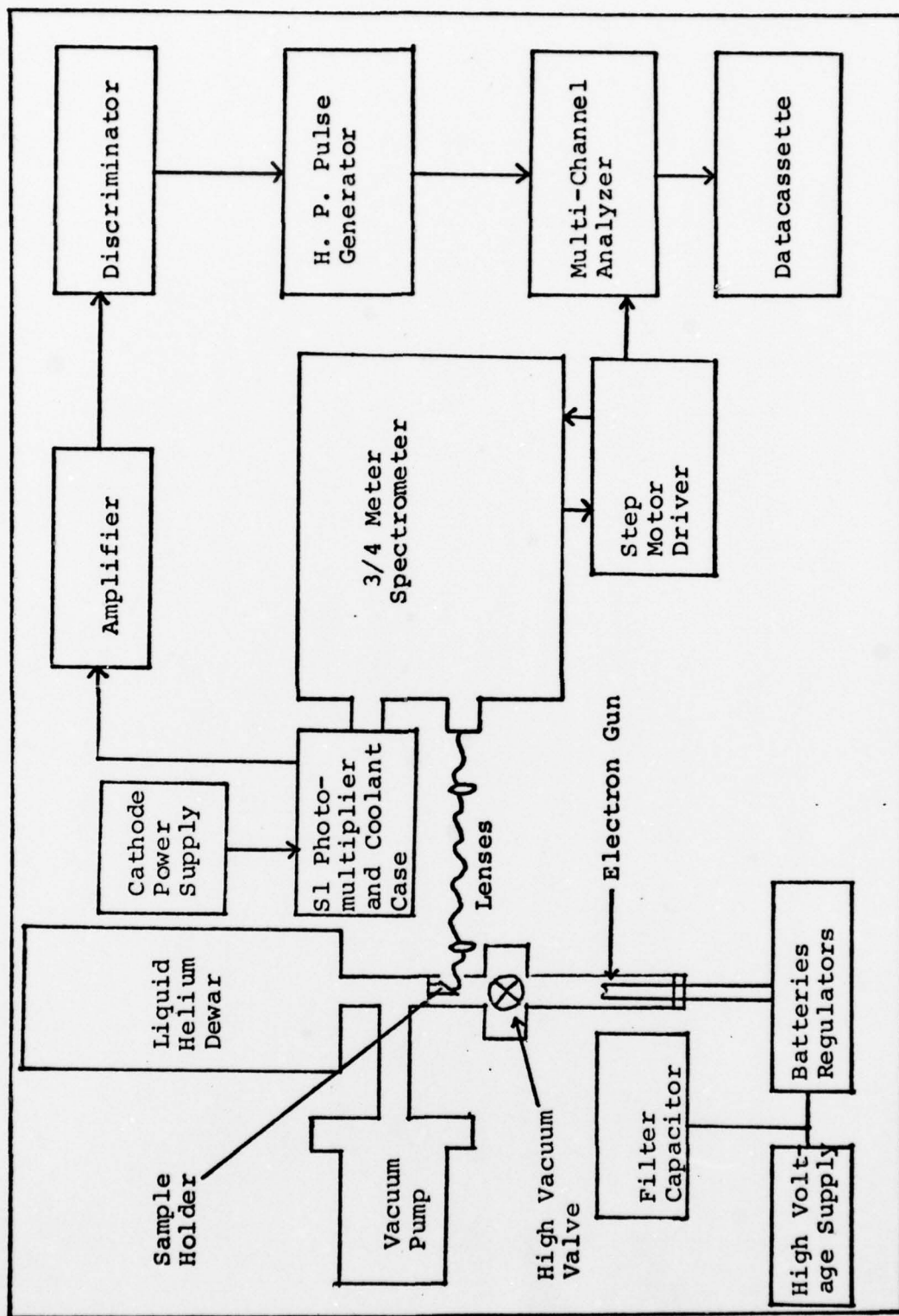The vacuum was maintained by a Welch Scientific Company series 3102D
turbo-molecular pump and was monitored by a Varian ionization gauge
with a Granville-Phillips ionization gauge controller.

The samples were cooled by liquid nitrogen or liquid helium
using an Andonian Associates model MHD-3L-30N liquid helium dewar.
Sample temperatures were measured by a precisely calibrated GaAs ther-
mometer, and typically reached $80^{\circ}K$ when liquid nitrogen was used and
$10^{\circ}K$ when liquid helium was used.

The samples were mounted on a copper sample block attached to the
end of the liquid helium dewar. The face of the copper block was cut
at a 45° angle to allow the vertical beam of electrons to strike the
samples. The face of the sample block was also oriented at a 45° angle
with respect to the optical axis of the spectrometer. Four samples
were simultaneously mounted on the face of the sample block with each
sample held in place by a copper mask with a small hole in it (Ref 3:
21). This allowed the luminescence from the implanted region of each
sample to be studied without the luminescence from the unimplanted
edges of the sample. The GaAs thermometer was located on the side
of the sample holder, and a Faraday cup, which was used to measure
the electron beam current, was mounted on its base (Ref 33:77). The
voltage from the thermometer was monitored by a Systron Donner model
7000A digital multimeter and the beam current was measured by a
Keithley 610A electrometer.

Excitation Source. The samples were bombarded by a beam of
energetic electrons from a Superior Electronics model 5A ZP4 electron
gun mounted vertically below the sample chamber. A high vacuum valve

was located above the gun so that it could be isolated in a vacuum during sample changes. The gun consists of a filament, cathode, two grids, and an anode. Bias voltages for the gun were supplied by a resistor chain isolated in a plexiglas box below the gun and connected between the negative high voltage output of a Universal Voltronics BAC 50-16 high voltage supply and ground. A 0.15 microfarad filter capacitor was connected in parallel with the resistor chain to maintain voltage stability. Below this plexiglas box was another plexiglas box containing a 12-volt automotive battery and a current regulator to supply current to the filament (Ref 12:16).

Since the sample block and the positive high voltage were connected to ground and the cathode was essentially at the potential of the high voltage supply, the energy of the electron beam was taken to be equivalent to the voltage reading of the high voltage supply. The maximum beam energy obtainable from this system was 25 kilovolts since at 27 kilovolts high voltage breakdowns occurred within the gun chamber (Ref 33:77).

The electron beam was directed on the sample to be studied or into the Faraday cup by the use of small permanent magnets which were placed on a 7 1/2 by 9 inch plexiglas platform located on top of the high vacuum valve.

Detection System. The luminescence produced in the samples was collected and focused onto the entrance slit of the spectrometer by two biconvex glass lenses. The first lens had a 10 centimeter focal length and was located approximately 10 centimeters from the samples. The second lens had a 20 centimeter focal length and was located approximately 20 centimeters in front of the entrance slit of the

21

spectrometer. Both lenses were mounted on a 50 centimeter optical bench so that they could each be moved in three mutually perpendicular directions. A Spectracoat Varipass filter which transmits 80% of the radiation above 6500Å, was located in the second lens mount to reduce the amount of light from the electron gun reaching the spectrometer.

A Spex model 1702 3/4 meter Czerny-Turner scanning spectrometer equipped with a Bausch & Lomb 600 grooves/millimeter grating blazed at 1.3 micrometers was used to examine the luminescence. With this grating, the wavelength counter reading was half of the true wave length being observed. The wavelength as measured by doubling the counter reading was found to be approximately 0.2 angstroms high. The scanning rate of this spectrometer could be adjusted from 0.5 to 5000 angstroms/minute (as read on the wavelength counter). The spectrometer could also be driven externally by signals from a step motor driver designed and constructed by G. Gergal (Ref 13:18-19). The spectrometer slits had continuously adjustable widths from 6 micrometers to 3 millimeters with slit lengths of 2, 5, 10, 20, or 50 millimeters.

An RCA C70007A photomultiplier tube with S1 response was used to detect the luminescence. The tube was cooled to -50°C by a Products for Research, Inc. model TE-176-RF refrigerated chamber. The cathode bias of the tube was supplied by a Keithley Instruments model 246 high voltage supply.

Signal Recording System. The electrical pulses from the photomultiplier were amplified by a model 1121 amplifier-discriminator unit that was manufactured by Princeton Applied Research. The output

signal from the discriminator was used to trigger a Hewlett Packard model 8010A pulse generator. This way, each pulse from the discriminator generated one pulse from the pulse generator with the required pulse shape and amplitude. These pulses were then counted and recorded by a Canberra model 8100 multi-channel analyzer (MCA) with 4096 channels. The step motor driver that drove the spectrometer also provided signals to the MCA to advance the channels at the desired ratio. Once the data was recorded by the MCA, it was transferred to magnetic tape by the use of a Techtran Industries model 8410 data cassette.

Procedures

This section describes the procedures used to align the optics and to record the data.

Alignment of Optics. Although GaAs does not luminesce in the visible, alignment of the optics was made easier by the use of a 2 mW He-Ne laser. The laser was located in a convenient place, and the beam was reflected into the sample chamber by a small mirror mounted on the frame of the cathodoluminescence apparatus. The red light scattered from the sample was then traced through the two lenses and the image of the sample focused on the entrance slit of the spectrometer. In this way, the scattered light from any of the samples could be focused on the slit by turning the adjustment screws on the lens holders while the optical bench remained in one location. Next, the laser beam was turned off and the electron beam made to strike the sample. The spectrometer was then scanned to locate a peak. Once a peak was located, final adjustment of the lenses was made in order to maximize

the signal strength as indicated on the display of the multi-channel analyzer.

Data Recording. In preparation for the recording of data, the dewar was filled with liquid nitrogen or liquid helium and the filament current turned on.

While the sample and filament temperatures were stabilizing, the optics were aligned with a He-Ne laser using the procedure described above. After the sample temperature had stabilized and the alignment procedure was completed, the slit widths were set to 100 microns, the argon lamp was turned on, and the wavelength counter of the spectrometer was set. To start the run, the spectrometer was set to external drive, and the multi-channel analyzer was placed in the "Collect" mode. After observing the recording of the reference line, the lamp was removed from in front of the entrance slit and the slits were increased to the setting to be used. The run was terminated when the multi-channel analyzer automatically switched to "Display". The data was then transferred to magnetic tap which was later used in a computer program to plot the graphs appearing in this thesis.

IV. Results and Discussion

In this experiment, the cathodoluminescence from six samples was examined. One sample was unannealed, two samples were thermally annealed, and three samples were laser annealed. Table II lists sample numbers, implant dosage, and type of annealing for each sample. The samples studied were chromium-doped, bulk-grown samples. Tellurium ions were implanted with a 120keV ion beam at room temperature. The samples were oriented in the $\langle 100 \rangle$ direction during implantation. The thermally annealed samples were capped with Si_3N_4 and annealed at $900^{\circ}C$ for 15 minutes in an atmosphere of flowing argon gas. The laser annealed samples were annealed at room temperature with a Q-switched Holobeam series 300 ruby laser. The laser beam energy densities for the laser annealed samples are also listed in Table II.

The spectra from the samples listed in Table II are presented in the following sections. First, the spectra obtained from the thermally annealed samples are presented. A portion of this data was recorded by Dr. Robert L. Hengehold prior to the beginning of this study. Second, spectra from an unannealed sample implanted to a fluence of $10^{13}/cm^2$ are presented. Finally, each of the spectra from the laser annealed samples are compared with the previous data to determine the effect of laser annealing.

The peak energies are considered accurate to within $\pm 1 meV$. This error is primarily due to the fact that each multi-channel analyzer is equivalent to $1.736 \overset{\circ}{A}$ of the spectrometer scan.

Thermally Annealed Samples

Typical Spectra 10^{13} Fluence. Typical spectra from sample 22 at

Table II

Samples Studies

Sample Number	Fluence ions/cm^2	Thermal Annealed	Unannealed	Laser Annealed	Energy Density J/cm^2
22	10^{13}	X			
23	10^{14}	X			
50	10^{13}		X		
10A	10^{13}			X	0.6
12A	10^{13}			X	0.804
15A	10^{13}			X	0.0716

10°K and 77°K are shown in Figure 6. The first peak appears at 1.514eV and 1.507eV at 10°K and 77°K respectively. If the band-gap energy is taken to be 1.521eV at 10°K and 1.514eV at 77°K (Ref 35:770), this peak is approximately 7meV below the band-gap energy at both temperatures. The data at 77°K and 10°K are not plotted on the same scale. Although the peak appears to have increased in intensity, it has actually de-creased slightly at 77°K. An investigation of the peak energy with changes in electron beam energy showed that the peak does not shift with changes in beam energy. If this peak were due to a free-bound transition, Eq (1) shows that as the temperature is raised to 77°K, the band-gap energy decreases 7meV, the KT/2 term would increase 3meV and the peak energy would increase 3meV with respect to the band-gap energy. Since the peak remains 7meV below the band-gap energy for all
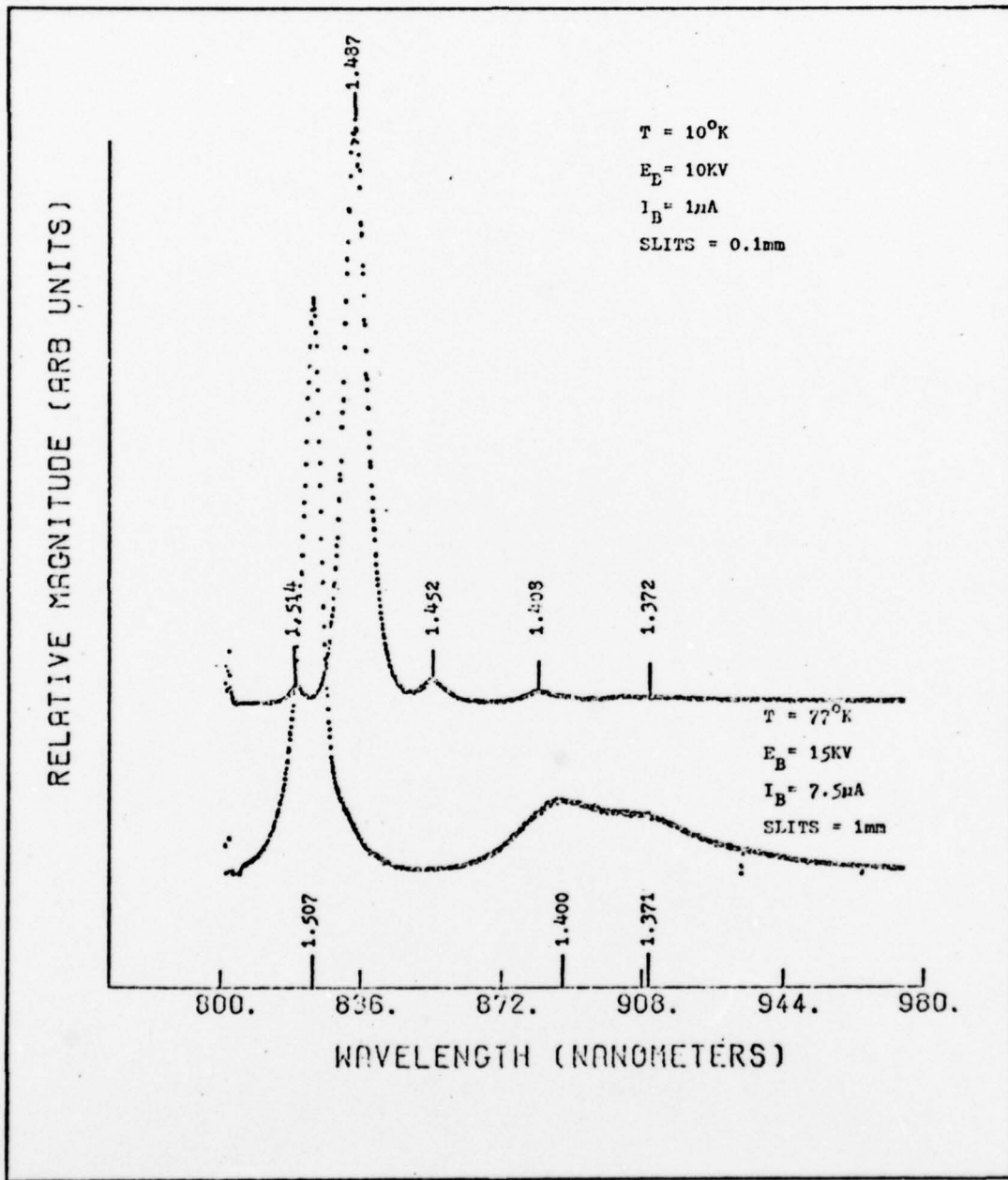
Figure 6. Typical Spectra of Thermally Annealed Sample 22 at 10°K and 77°K

temperatures and beam energies investigated and does not shift with temperature as a free-bound recombination would, it is attributed to the recombination of an exciton. Bogardus (Ref 2) has identified a peak at 1.5156eV (at 2°K) as a transition from a free exciton. It is believed that this is the same peak and that the 1.6meV difference in peak position is due to the temperature shift of the band-gap energy from 2°K to 10°K.

The second peak occurs at 1.487eV at 10°K and does not appear at 77°K. The peak energy was examined for a dependence on excitation intensity. Since the beam area remained constant, an increase in beam energy is also an increase in excitation intensity. Figure 7 shows the spectra at 10°K with beam energies of 5 and 2.0 kilovolts. There appears to be a shift in this peak toward lower energies as the excitation intensity is decreased. Table III lists the peak energies measured from a complete series of spectra recorded at 10°K. The plots in Figure 7 are a part of this series. The data in Table III shows that the exciton peak energy remains fairly constant at all beam energies. The intensity of this peak became too low to detect at beam energies below 3kV and, hence, the bottom of the column is filled with dashes. The 1.487eV peak has been labeled as a donor-acceptor peak for reasons that will be explained. This peak shows a definite shift toward higher energies as the excitation intensity increases. Using the peak of the LSS curve in Figure 3 and referring to the peak position vs. dopant curve in Figure 2, the shift in this peak would not be expected if it were associated with a free-bound transition.

A curve for donor-acceptor recombinations with increasing donor concentration is not shown in Figure 2; however, the top curve shows
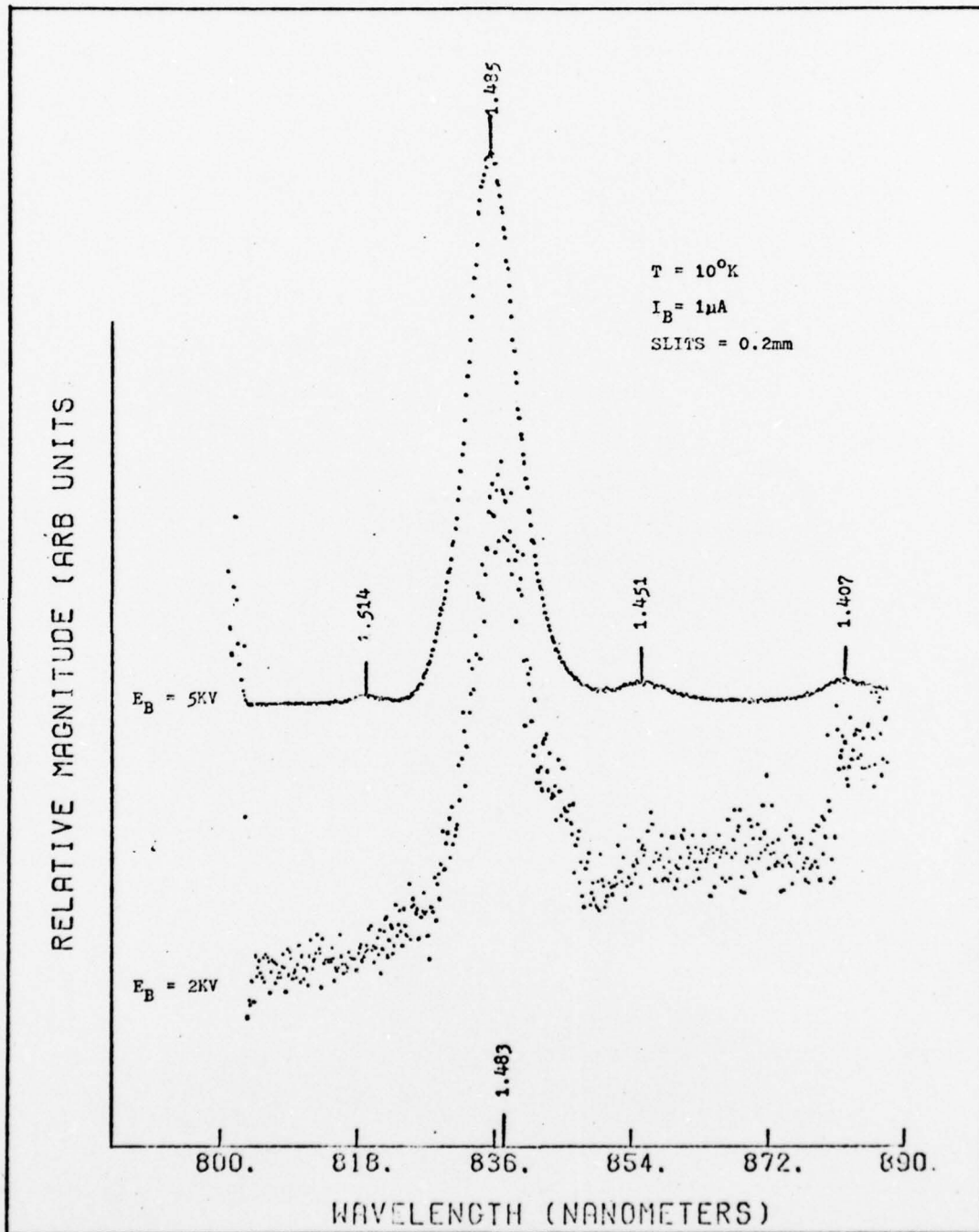
Figure 7. Spectra of Thermally Annealed Sample 22
at 5kV and 2 kV

29

Table III

Peak Energy vs Beam Energy Sample 22

Temperature: 10°K

Beam Energy (KV)	Exciton Peak Energy (eV)	Donor-Acceptor Peak Energy (eV)
10.0	1.514	1.487
7.5	1.514	1.486
5.0	1.514	1.485
4.5	1.514	1.485
3.85	1.514	1.485
3.8	1.514	1.485
3.75	1.514	1.484
3.5	1.513	1.484
3.0	1.514	1.484
2.5	-	1.484
2.25	-	1.483
2.0	-	1.482
1.9	-	1.482

that the energy of the bound electron is increasing. This change in the energy of the bound electron will cause donor-acceptor peaks to shift toward higher energies. Table III shows that the 1.487eV peak shifts toward higher energies (indicating a high concentration of Te) as the beam energy is increased. However, the electrons (as shown in Figure 4) penetrate deeper into the crystal with an increase of beam

energy. Thus, as the electrons probe deeper into the crystal, higher concentrations of Te are present at depths well past the implant layer (as shown by Figure 3). This does not make physical sense, so the shift in peak energy is not due to banding.

However, increasing the excitation intensity will favor the closer donor-acceptor pairs and a donor-acceptor peak will shift toward higher energies (Ref 13:791, 38:335-6). Since this peak was not present at $77^{O}K$, the intensity of this peak decreased with an increase in temperature. Bogardus and Bebb (Ref 2) observed that donor-acceptor peaks decrease rapidly in intensity with increasing temperature. Based on the arguments presented and the fact that this peak is dominant in Te-doped samples, the 1.487eV peak at $10^{O}K$ in Figure 6 is attributed to a Te donor-acceptor transition.

The transitions discussed above are due to recombinations involving simple centers. Recombinations involving two complex centers are shown in Figure 6 at 1.408eV and 1.400eV at $10^{O}K$ and $77^{O}K$ respectively. These peaks appear near luminescent lines that have been identified as involving As vacancies (Ref 4:144). Thus it was believed that these peaks are associated with As vacancies.

Another recombination involving a complex center is at 1.372eV and 1.371eV at $10^{O}K$ and $77^{O}K$ respectively. Chiang and Pearson (Ref 7) observed that emission peaks near 1.37eV only appeared in samples when they had been annealed in ampoules made of quartz containing traces of copper. In agreement with Chiang and Pearson, the 1.372eV peak and the 1.371eV peaks are attributed to copper contamination of the sample.

One additional peak appearing in Figure 6 has not been identified. The peak at 1.452eV at $10^{O}K$, which is not present at $77^{O}K$, is 35meV

below the donor-acceptor peak. Since the energy of the longitudinal optical (LO) phonon is approximately 36meV in GaAs (Ref 19:829, 38:38), the 1.452eV peak is considered to be a LO phonon replica of the donor-acceptor peak. The 1meV difference in energy is attributed to the accuracy of the measurements of the peak energies as noted at the beginning of this chapter.

Typical Spectra 10^{14} Fluence. Typical spectra from sample 23 at 10°K and 80°K are shown in Figure 8. As with sample 22, there is a peak at 1.514eV and 1.507eV at 10°K and 80°K respectively. This peak again remains approximately 7meV below the band-gap for all temperatures and beam energies used and decreases in intensity as the temperature increases. In agreement with sample 22, this peak was attributed to a recombination involving a free exciton.

The 1.488eV peak at 10°K is 33meV below the band-gap and does not appear in the spectrum at 80°K. This peak energy was investigated for a dependence on excitation energy. Figure 9 shows the spectrum at 10°K obtained with beam energies of 5 and 1.8 kilovolts. The same shift that was observed with the donor-acceptor peak in the spectrum of sample 22 was again observed. Table IV lists the peak energies measured from a complete series of spectra recorded at 10°K. The plots in Figure 9 are a part of this series. As with sample 22, the exciton peak energy remains constant for all beam energies. The intensity of this peak was again too low to detect at beam energies below 2.5 kilovolts. The donor-acceptor peak shows a definite shift towards higher energies as the beam intensity increases. Based on this data, the dominant peak at 10°K was attributed to a Te donor-acceptor transition in agreement with the discussion of sample 22.
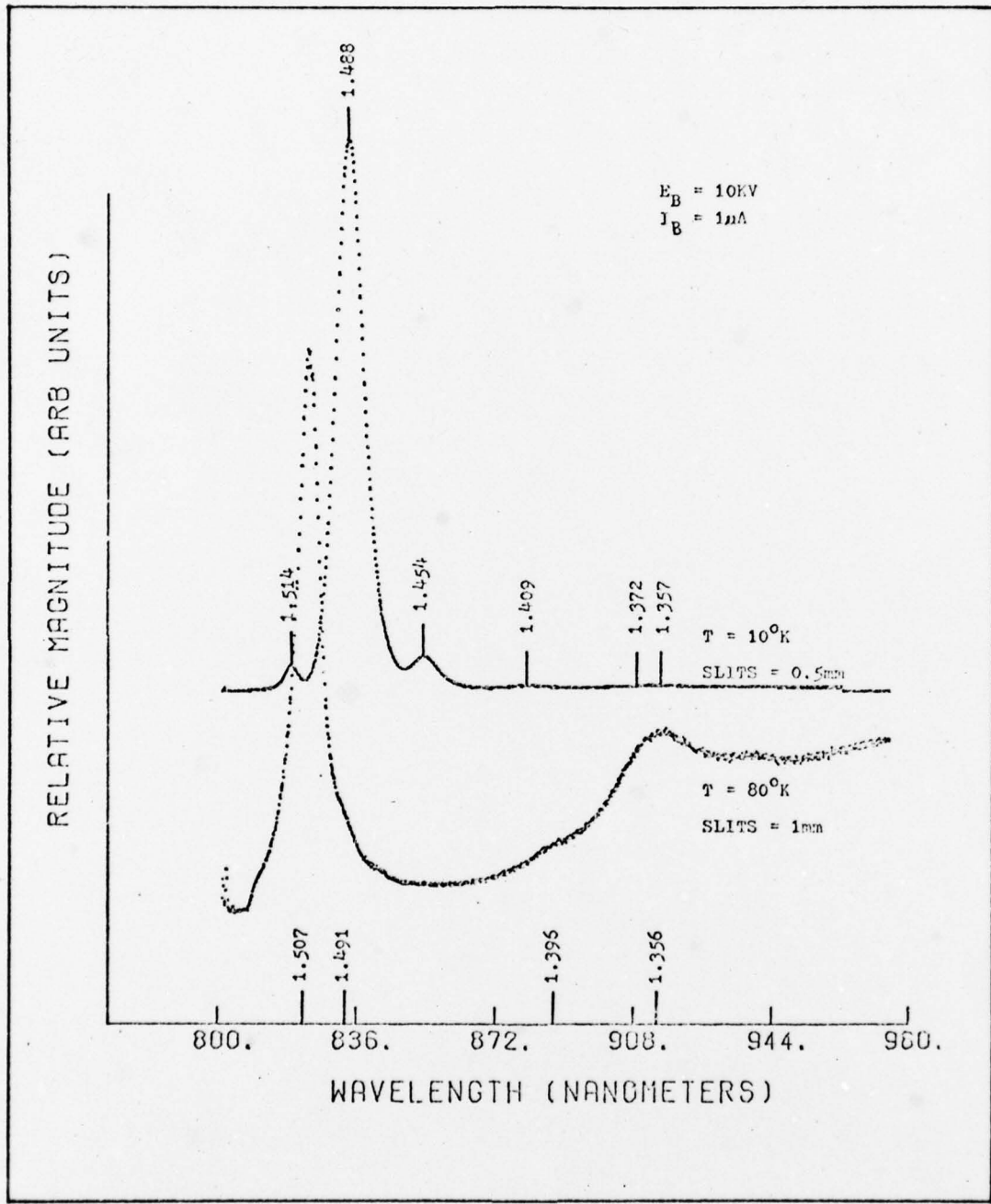
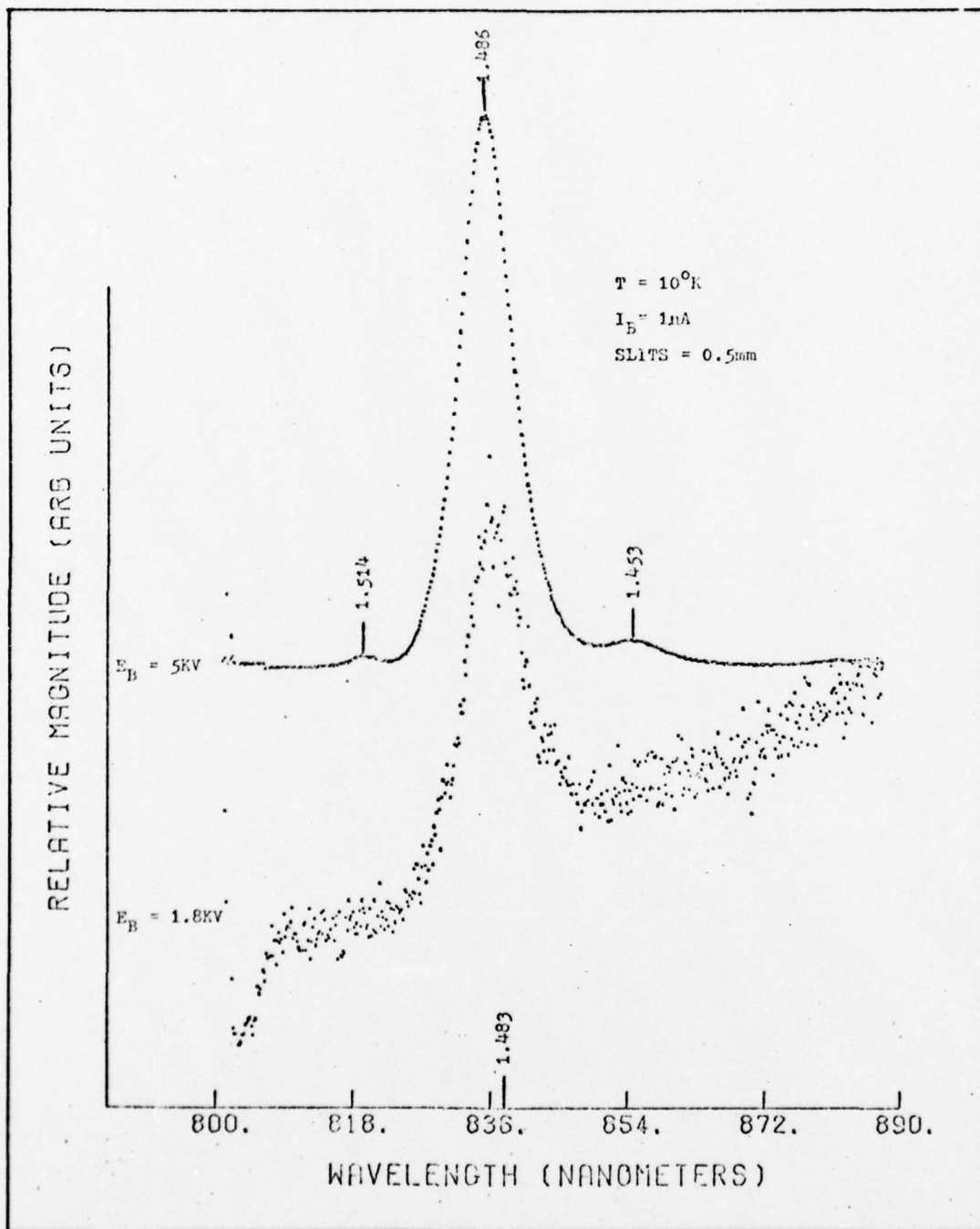Figure 8. Typical Spectra of Thermally Annealed Sample 23
at 10°K and 80°K

Figure 9. Spectra of Thermally Annealed Sample 23
at 5kv and 1.8kv

34

Table IV

Peak Energy vs Beam Energy Sample 23

Temperature: 10°K

Beam Energy (KV)	Exciton Peak Energy (eV)	Donor-Acceptor Peak Energy (eV)
20.0	1.514	1.488
10.0	1.514	1.488
7.5	1.514	1.487
5.0	1.514	1.486
4.5	1.514	1.486
3.5	1.514	1.486
2.5	1.514	1.485
2.0	-	1.484
1.8	-	1.484
1.7	-	1.483

The fact that this peak is not present at 80°K is due to the fact that the intensity of the donor-acceptor peak has decreased as the donors have become ionized with the temperature increase. When Bogardus and Bebb (Ref 2:996) observed a decrease in intensity in the donor-acceptor peak, an increase in intensity was observed in a band-acceptor peak. There is a shoulder in the spectrum at 80°K in Figure 8 at 1.491eV. Since this was the only spectrum where this peak was observed, it was not possible to observe the peak energy with changes in temperature

or beam energy. Due to the fact that this peak did not appear until the donor-acceptor peak intensity was too low to detect, the 1.491eV peak at 80°K is attributed to a conduction band-acceptor recombination. The shift from a donor-acceptor peak at 10°K to a conduction band-acceptor peak at 80°K is due to the donors becoming ionized and the electrons being funneled into the band-acceptor peak.

All of the remaining peaks in Figure 8 except the 1.357eV peak at 10°K and the 1.356eV peak at 80°K are considered to be the same as the corresponding peaks described for sample 22. As the temperature was raised from 10°K to 80°K, the 1.357eV incrased 7meV with respect to the band-gap energy. Although an investigation for a dependence on excitation intensity was made, no clear trend was observed. A 1.35eV peak was observed by Chatterjee et al (Ref 6) when outdiffusion of Ga was enhanced by annealing with a SiO_3 cap. Innagreement with this finding, it is velieved that the 1.35eV peak at 10°K and the 1.356eV peak at 80°K are the same peak and are due to the presence of Ga vacancies.

There are two main differences in the spectrum of samples 22 and 23. First, the donor-acceptor peak appears to have shifted to higher energies with the 10^{14} fluence sample 23. Figure 10 shows some of the data taken from Tables III and IV. This figure and the rest of the data from these two tables show that the donor-acceptor peak in sample 23 has shifted towards higher energies for all beam energies. Second, the appearance of the Ga vacancy peak was observed in sample 23. Since the annealing conditions were the same for both samples, this might indicate that more damage to the crystal lattice was caused during ion implantation with the higher fluence.
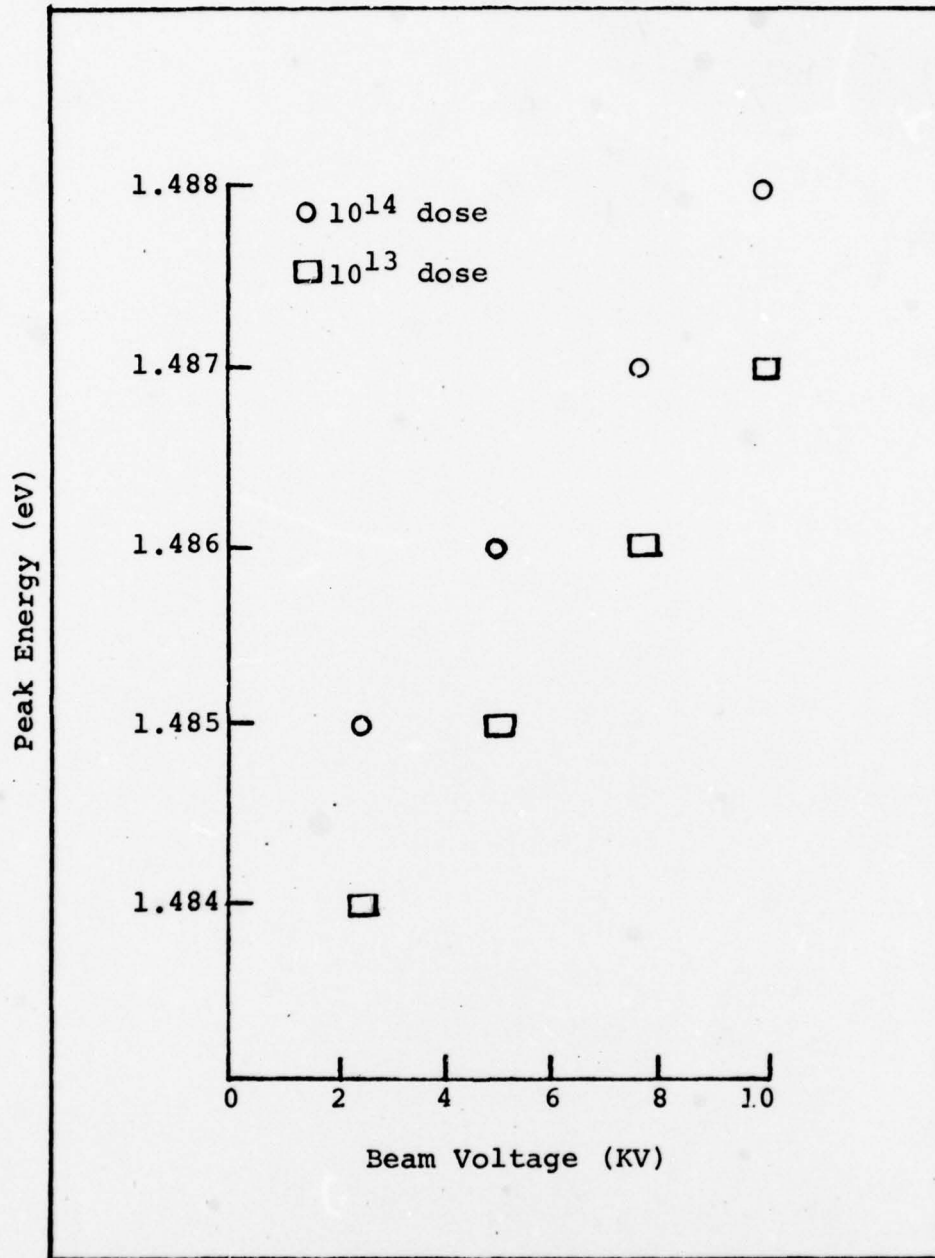
Figure 10. Comparison of Donor-Acceptor Peak Energy

Unannealed Sample

Typical spectra of the implanted but unannealed sample 50 is shown in Figure 11 at 10°K and 77°K. This first peak occurs at 1.514eV and 1.505eV at 10°K and 77°K respectively, and decreases 3meV with respect to the band-gap energy at a temperature of 77°K. This shift in peak energy is in a direction opposite to the shift for a free-bound transition as discussed in Chapter II. The graphs in Figure 11 were not plotted on the same scale. Although the peaks appear to have increased in intensity, it has actually decreased slightly at 77°K. Additionally, the peak energy was investigated for a dependence on excitation intensity, but no clear evidence was observed. Bogardus and Bebb (Ref 2) have observed the luminescence from excitons bound to neutral and ionized donors. They observed peaks with approximately the same energy as the 1.514eV peak which shifted to lower energies as the donor became ionized. Two other factors should be considered before determining the source of this peak. The sample is unannealed and has undergone ion-implantation which creates lattice damage. Pankove (Ref 32:124) observed that with less perfect crystals local fields tend to break up the excitons into free carriers. Therefore, although the peak shifts like a bound exciton with changes in temperature, the existence of excitons in the spectrum of a crystal containing lattice damage seems unlikely. However, referring to the LSS curve shown in Figure 3, it can be seen that the Te implanted layer is approximately 800Å thick. The electron excitation profile shown in Figure 4 shows that the majority of the radiation is coming from a region below the implanted layer. Hence, it is believed that the 1.514eV peak at 10°K (1.505eV at 77°K) is due to the recombination of a bound exciton. Further,

RELATIVE MAGNITUDE (ARB UNITS)

1.491

T = 10°K

E$_B$= 10KV

I$_B$= 7μA

SLITS = 1mm

1.514

1.470

1.454

T = 77°K

E$_B$= 15KV

I$_B$= 7.5μA

SLITS = 1.5mm

1.505

800.   836.   872.   908.   944.   980.
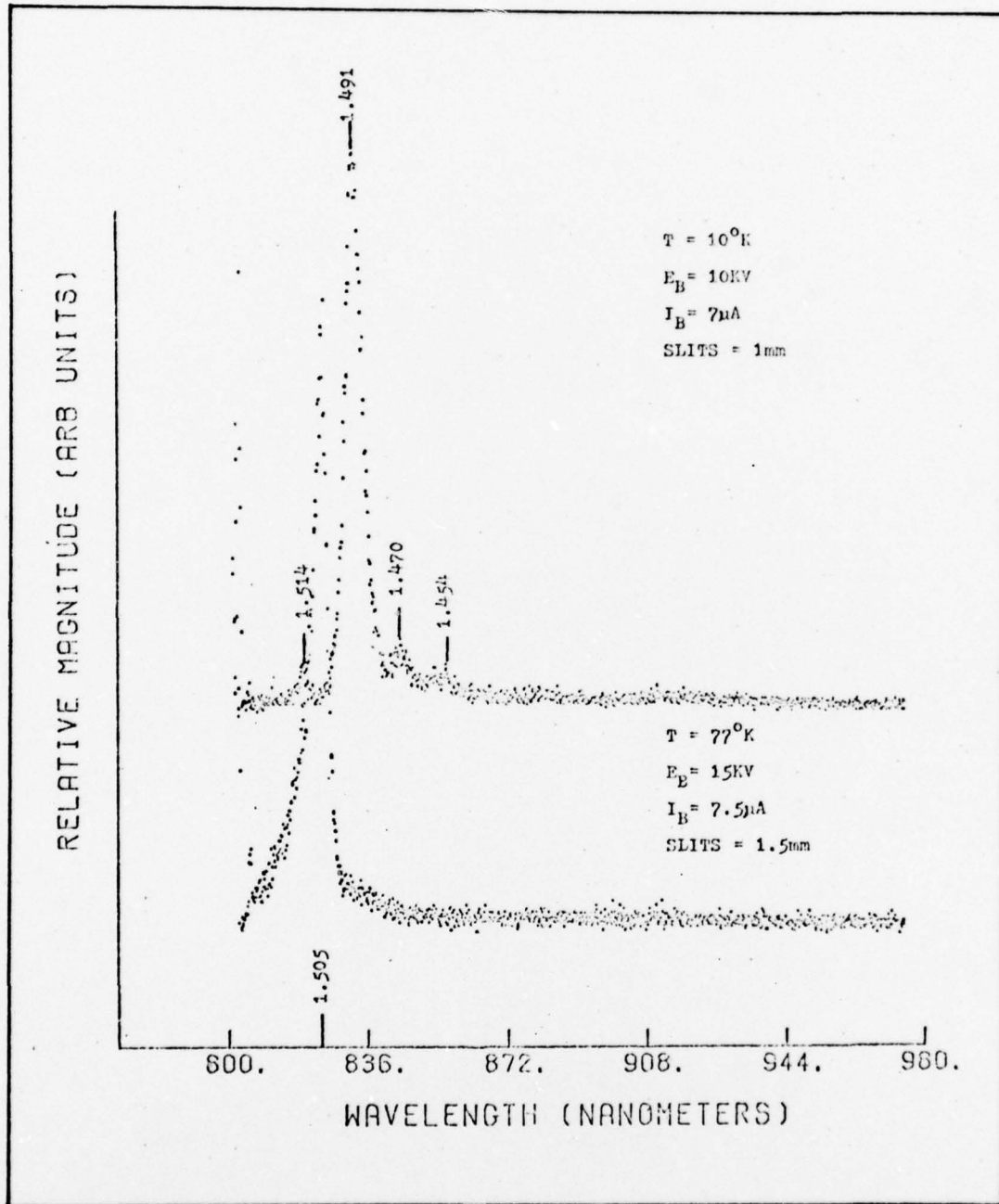
WAVELENGTH (NANOMETERS)

Figure 11. Typical Spectra of the Unannealed Sample
at 10°K and 77°K

the majority of the radiation is coming from the substrate below the implanted layer and the low intensity of the peak is due to the radiation being absorbed by the amorphous, implant layer.

The second peak appears at 1.491eV at 10°K and is not present at 77°K. Although this is the dominant peak, its intensity is very weak and is only 1/60 the number of counts as in the donor-acceptor peaks observed in the thermally annealed samples. This peak appears 30meV below the band-gap energy. Due to a limited amount of data available, it was not possible to observe the dependence of the peak energy on beam energy. Two possible explanations are presented for this peak. First, this is the same Te donor-acceptor peak observed in the spectra of sample 22; however, it has shifted 4meV towards higher energies. This shift would indicate a change in the donor and/or acceptor binding energies due to lattice structure damage during ion-implantation. Second, the peak is due to a conduction band-acceptor recombination. The fact that the peak intensity has decreased rather than increased with an increase in temperature would be due to the damage to the lattice caused during ion implantation. At the warmer temperatures the carriers are shifting to non-radiative recombinations at defect sites. Without observing the peak energy with changes in beam energy or small changes in temperature, it is not possible to positively identify the origin of this peak. However, Ashen (Ref 1) has attributed peaks near 1.49eV at 5°K to either a band-carbon acceptor transition or a band-zinc acceptor transition. Therefore, it is believed that the 1.491eV peak is a conduction band-acceptor transition. The intensity of this peak decreased rather than increased at warmer temperatures as the luminescence was being quenched by

non-radiative recombinations.

The 1.470eV peak at 10°K is 51meV below the band-gap energy and is not present at 77°K. Chatterjee, et al, have observed that this peak is present in GaAs when As outdiffusion is enhanced (Ref 5:568, 6:1422). In agreement with Chatterjee, the 1.470eV peak was attributed to an As vacancy.

The final peak in the spectra at 10°K appears at 1.454eV and is extremely weak. This peak is 37meV below the 1.491eV peak. Since this difference in peak energy is approximately equal to the energy of a LO phonon, the 1.454eV is attributed to a phonon replica peak.

Laser Annealed Samples

Sample 10A. The spectra obtained from sample 10A at 24°K and 77°K are shown in Figure 12. As with the spectra from the unannealed sample, the intensities of the peaks are very weak. A comparison of Figure 12 with Figure 11 reveals that the spectra of the laser annealed sample is almost identical to the spectra of the unannealed sample.

The first peak appears at 1.514eV and 1,506eV at 24°K and 77°K respectively and has decreased in intensity at 77°K. If the band-gap energy is taken to be 1.520eV at 24°K and 1.514eV at 77°K (Ref 35:770), the peak energy decreased 2meV with respect to the band-gap energy as the temperature was increased. An examination of the peak energy vs beam energy was not possible as the spectra was only detectable with the maximum beam energy available, i.e. 15 kilovolts. As with the unannealed sample, the peak shifts with changes in temperature in a manner similar to an exciton bound to a donor which becomes ionized with an increase in temperature, so this peak is attributed
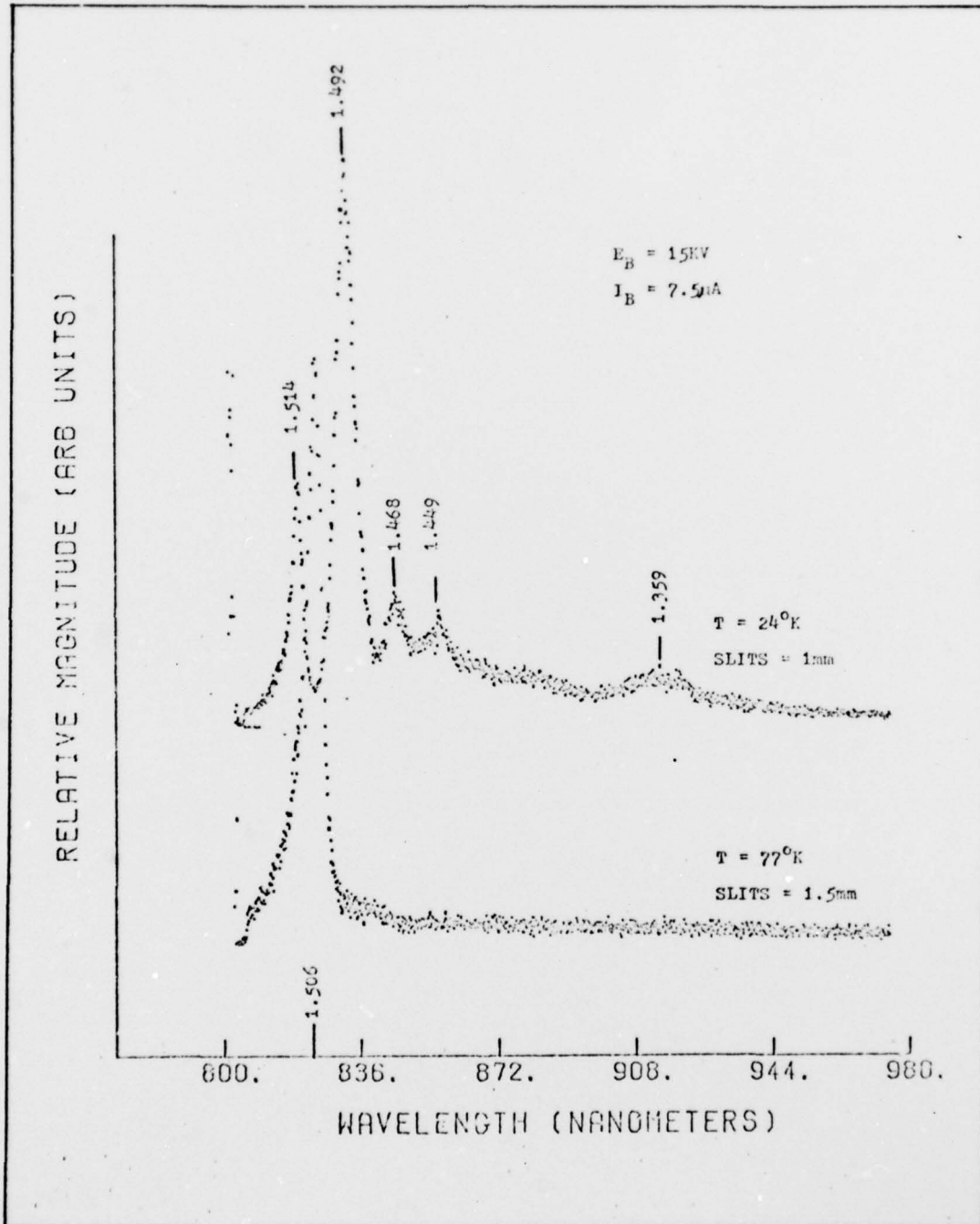
41

Figure 12. Spectra of Laser Annealed Sample 10A
at 24°K and 77°K

to the recombination of a bound exciton.

The dominant peak in the spectra in Figure 12 is not the 1.487eV Te donor-acceptor peak but a peak 5meV higher in energy. The 1.492eV peak at 24°K is less than 1/30 the intensity of the Te donor-acceptor peak and is not present in the spectra at 77°K. An examination of the peak energy vs beam energy was not possible as the peak appeared only when a 15KV beam voltage with a 7.5μA beam current was used. Since the peak shape and intensity are very similar to the band-acceptor peak in the spectra of the unannealed sample and since there is only a 1meV difference in peak energies, the 1.492eV peak is considered to be a conduction band-acceptor transition. The 1meV difference in peak energies is attributed to the accuracy of the experimental measurements noted earlier.

The 1.468eV peak and 1.359eV peak have been previously discussed and are again attributed to As and Ga vacancies respectively.

The final peak occurs at 1.449eV, which is 71meV below the band-gap energy. This peak is too far below the band-gap to be due to a simple center and the energy of the peak does not correspond to the energy of complex centers from Ga or As vacancies. Without additional information, it is not possible to identify the cause of this peak and it is, therefore, labeled "unknown".

The absence of the Te donor-acceptor peak indicates that the Te ions have not moved to substitutional sites and annealing has not occurred.

It should also be noted that no luminescence was observed for beam energies below 15kV and the spectra observed at 15kV is essentially the same as that obtained from the unannealed sample. The LSS profile

in Figure 3 indicates that the implanted layer is approximately 800Å thick. Since no luminescence was observed with beam energies below 15kV, the electron excitation profiles in Figure 4 indicate that no luminescence is being observed from the first 5000Å of the crystal but rather from a deeper layer in the crystal.

One possible cause for the quenching of the luminescence is that a layer near the surface is being severely damaged by the laser. The laser radiation is being absorbed in this layer and the dominant recombinations are non-radiative rather than radiative. Another possible cause is that an oxide or Ga_2Te_3 layer is being formed on the surface and is absorbing the luminescence before it can leave the crystal. Since the observed luminescence is nearly identical to that from an unannealed sample rather than an annealed sample with lower intensities, it is believed that a layer near the surface including the implanted layer is being severely damaged by the laser radiation.

Sample 12A. The spectrum obtained from the laser annealed sample 12A at 77°K is shown in Figure 13. The spectrum from the thermally annealed sample 22 is provided for comparison. The spectrum from the laser annealed sample appears to be identical to that of the unannealed sample at 77°K which is shown in Figure 11. A single peak appears at 1.505eV, 2meV below the exciton peak in the thermally annealed samples and 9meV below the band-gap energy. If this peak is due to a donor-valence band transition, Eq (1) indicates that with a KT/2 term of 3meV (Ref 3:7), the donor binding energy would be approximately 12meV which is a value twice as high as the energies for donors that have been measured in GaAs (Ref 39:328-329); hence, the peak is not due to a donor-band recombination. It should be noted that the intensity of
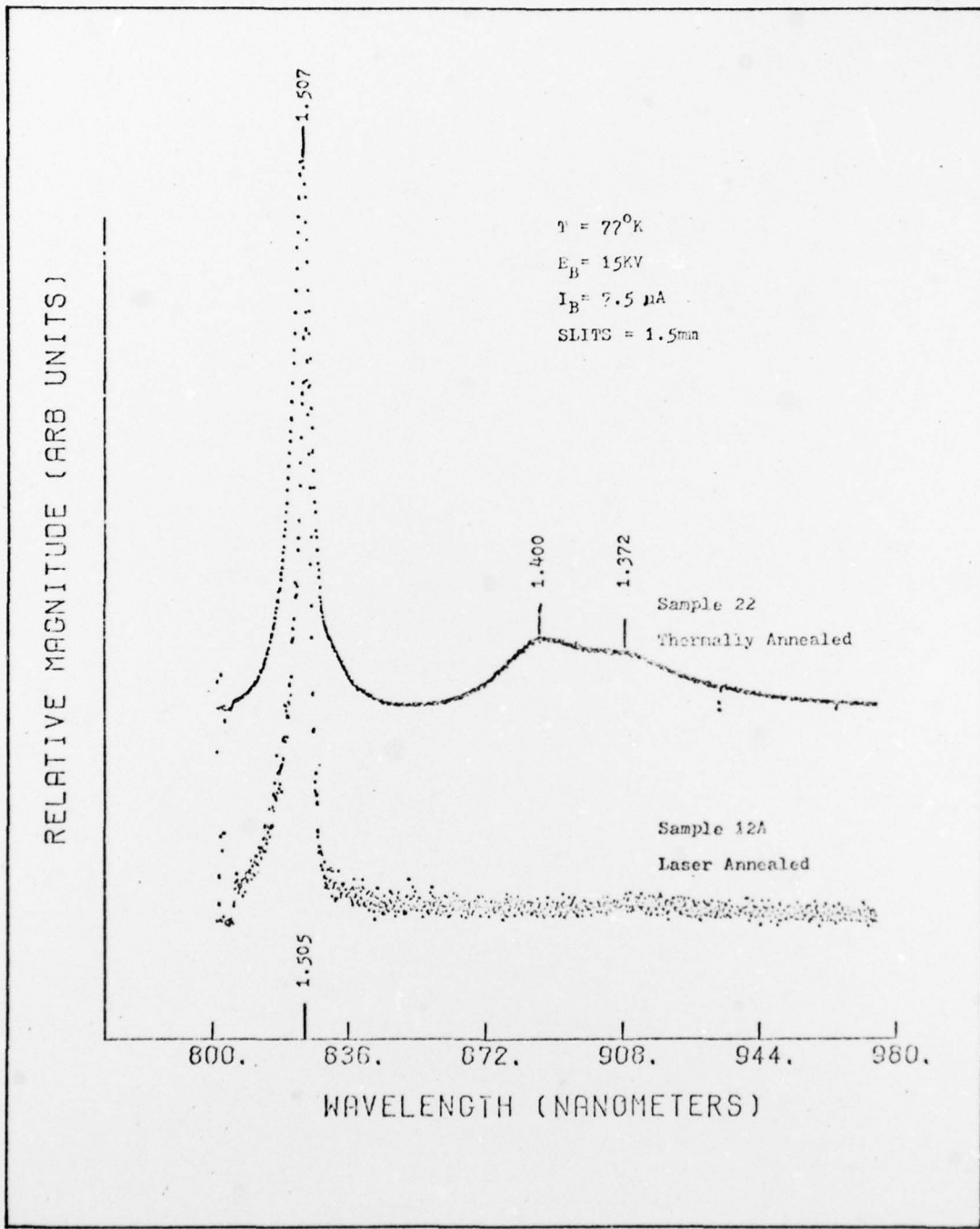
Figure 13. Spectra of Sample 12A and 22
at 77°K

45

this peak is the same as that of the 1.505eV damage peak in the spectra of the unannealed sample which is less than 1/6 the intensity of the exciton peak of sample 22.

As with sample 10A, the luminescence was not detected until the maximum beam voltage was used, and then the luminescence that was detected was identical to that of the unannealed sample. It appears that as with sample 10A, the laser radiation is being absorbed in a layer near the surface of the crystal and that this layer is being severely damaged. The absence of the 1.400eV and the 1.372eV peak is due to one of two causes. The luminescence is present, but being absorbed by the damage layer, or the peaks are not present as in the unannealed sample. In either case, a layer near the surface, including the implant layer, is being damaged by the laser radiation.

Sample 15A. The spectrum obtained from the laser annealed sample 15A is presented in Figure 14 along with the spectrum from the thermally annealed sample 22 at $10^{\circ}K$.

The first peak appears at 1.487eV which is 1meV higher in evergy than the donor-acceptor peak in the spectra of sample 22. Since this was the only spectrum recorded of this sample, the 1.487eV peak is attributed to a Te donor-acceptor peak on the basis of peak position. The difference in peak energy is due to the higher beam energy used. Although the beam current was 4.4 times higher, the intensity of this peak was only 1/25 the intensity of the 1.486eV peak in sample 22.

The absence of the 1.451eV LO phonon peak is due to the weak intensity of the 1.487eV no-phonon peak.

As with both the unannealed and thermally annealed samples, an As vacancy peak (1.466eV) is present. The presence of the 1.354eV
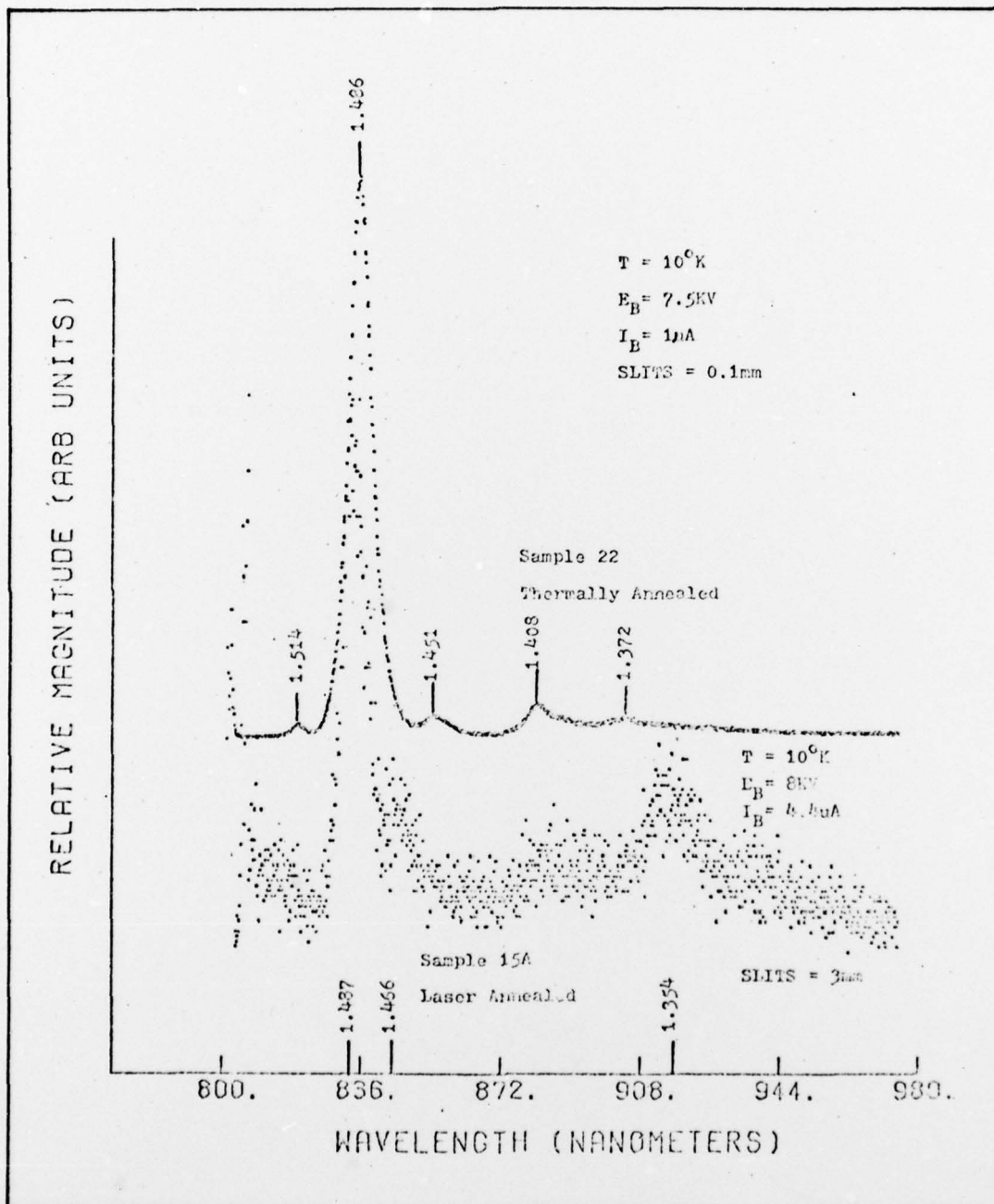
46

Figure 14.   Spectra of Sample 22 and 15A
at 10°K

47

Ga vacancy peak (Ref 6) which was not observed in the unannealed sample indicates that the laser has created Ga vacancies.

The exciton peak (1.514eV) is not present in the spectrum of the laser annealed sample. Using Pankove's argument that, with less perfect crystals, excitons break up into free carriers, it is believed that enough heating has not occurred to recrystallize the implanted layer.

The above data indicates that some of the Te ions have moved to substitutional sites; however, the weak intensity of the peaks and the absence of the exciton peak indicates that little heating and recrystallization of the implanted layer has occurred.

V. Conclusions and Recommendations

Conclusions

In this thesis, the cathodoluminescence spectra of Te implanted GaAs were studied. Based on the analysis of these spectra as presented in the preceding chapter, the following conclusions have been reached:

1. The 1.487eV peak at 10°K in Te implanted GaAs is a Te donor-acceptor recombination. This conclusion is based on the peak energy shift with changes in beam energy and on the change in intensity with changes in temperature.

2. The Te donor-accepor peak shifts to higher energies as the Te fluence is increased from 10^{13} to 10^{14} ions/cm^2.

3. When a laser energy density of 0.07 J/cm^2 was used (sample 15A), two conclusions were reached. First, only a small percentage of the Te ions moved to substitutional sites. This was based on the extremely weak intensity of the Te donor-acceptor peak. Second, the laser radiation created Ga vacancies that were not present in the unannealed sample.

4. When a laser energy density of 0.6 J/cm^2 or higher was used (samples 10A and 12A), the implant layer was damaged and all of the luminescence from that layer was quenched. Further, the luminescence was only detectable when the maximum electron beam energy available was used (i.e. 15kV) and the spectrum that was obtained was characteristic of the substrate, not the implanted layer.

Recommendations

The following recommendations are made concerning further studies and improvements to the cathodoluminescence apparatus:

1. Laser energy densities between 0.07 J/cm^2 and 0.6 J/cm^2 should be used and the samples studied to determine the annealing effect.

2. Examine the effect of using a pulsed Nd^{3+} Yag laser. Since the energy of the laser photons is less than the GaAs band-gap energy, the laser radiation will interact primarily with impurities and lattice defects rather than the bulk material.

3. The pulsing capability of the electron gun should be used so that time-resolved studies of the spectra at various depths within the sample can be made.

4. Electrical measurements should be made on the samples to test the conclusions of this thesis.

5. The helium dewar should be replaced with a Heli-Tran system to extend the experimental run time at helium temperatures beyond the dewar's 2 1/4 hour limit.

6. A mirror should be mounted between the electron gun and the sample chamber. During alignment of the optics this would allow the He-Ne laser beam to be directed onto the sample from below and the reflections off the sample chamber could be avoided.

7. The pulse capability of the electron gun along with the use of a Princeton Applied Research model 1112 photon counter/processor should be used to obtain spectra without the background black body radiation from the electron gun.

50

Bibliography

1. Ashen, D. J. et al. "The Incorporation of Characterization of Acceptors in Epitaxial GaAs," *Journal of Physics and Chemistry of Solids*, 36:1041-1053 (1975).

2. Bogardus, E. H. and H. Bebb. "Bound-Exciton, Free-Exciton, Band-Acceptor, Donor-Acceptor, and Auger Recombination in GaAs," *Physical Review*, 176:933-1002 (December 1968).

3. Boulet, D. L., Jr. *Depth Resolved Cathodoluminescence of Cadium Implanted Gallium Arsenide.* Unpublished thesis. Wright-Patterson AFB, Ohio: Air Force Institute of Technology, December 1975.

4. Chang, L. I. et al. "Vacancy Association of Defects in Annealed GaAs," *Applied Physics Letters*, 19:(5):143-145 (September 1971).

5. Chatterjee, P. K. et al. "Photoluminescence from Be-Implanted GaAs," *Applied Physics Letters*, 27(10):567-569 (November 1975).

6. -----. "Photoluminescence Study of Naitve Defects in Annealed GaAs," *Solid State Communications*, 17:1421-1424 (December 1975).

7. Chiang, S. Y. and G. L. Pearson. "Photoluminescence Studies of Vacancies and Vacancy-Impurity Complexes in Annealed GaAs," *Journal of Luminescence*, 10:313-322 (1975).

8. Colbow, K. "Free-to-Bound and Bound-to-Bound Transitions in CdS," *Physical Review*, 141(2):742-749 (January 1966).

9. Cone, M. L. *Cathodoluminescence Characterization of Ion Implanted GaAs.* Unpublished Dissertation, Wright-Patterson AFB, Ohio: Air Force Institute of Technology.

10. Cusano, D. A. "Identification of Laser Transitions in Electron Beam-Pumped GaAs," *Applied Physics Letters*, 7(6):151-152 (September 15, 1965).

11. -----. "Radiative Recombinations from GaAs Directly Excited by Electron Beams," *Solid State Communications* 2:353-358 (1964).

12. Daniels, C. R. *Pulsed Cathodoluminescence of Ion-Implanted ZnO.* Unpublished thesis. Wright-Patterson AFB, Ohio: Air Force Institute of Technology, March 1975.

13. Dingle, R. "Radiative Lifetimes of Donor-Acceptor Pairs in P-Type Gallium Arsenide," *Physical Review*, 184(3):788-796 (August 15, 1969).

14. Dumoulin, J. D. *Depth-Resolved Cathodoluminescence on the Effects of Cd Implantation and Annealing in Gallium Arsenide.* Unpublished thesis. Wright-Patterson AFB, Ohio: Air Force Institute of Technology, September 1974.

15. Gibbons, J. F. "Ion Implantation in Semiconductors--Part I Range Distribution Theory and Experiments," Proceedings of the IEEE, 56(3):295-318 (March 1968).

16. -----, et al. Projected Range Statistics. New York: Halsted Press, 1975.

17. Golovchenko, J. A. and T. N. C. Venkatesan. "Annealing of Te-Implanted GaAs by Ruby Laser Irradiation," Soviet Physics-Semiconductors, 12(2):147-149. (February 1978).

18. Harris, J. S. et al. "Influence of Implantation Temperature and Surface Protection on Tellurium Implantation in GaAs," Applied Physics Letters, 21(12):601-603 (December 15, 1972).

19. Hwang, C. J. "Evidence for Luminescence Involving Arsenic Vacancy Acceptor Centers in P-Type GaAs," Physics Review, 180:827-832 (April 1969).

20. -----. "Photoluminescence Study of Thermal Conversion in GaAs Grown from Silica Boats," Journal of Applied Physics, 39(12): 5347-5356 (November 1968).

21. Itoh, T. and M. Takeuchi. "Arsenic Vacancy Formation in GaAs Annealed in Hydrogen Flow," Japanese Journal of Applied Physics. 16(2)227-232 (February 1977).

22. Kachurin, G. A., et al. "Annealing of Defects in Ion-Implanted Layers," Proceedings of the Fifth International Conference on Ion Implantation in Semiconductors and Other Materials. 445-451. Plenum Publishing Corp., 1977.

23. -----. "Annealing of Radiation Defects by Laser Radiation Pulses," Soviet Physics-Semiconductors, 9(7):946 (1975).

24. -----.and E. V. Nidaev. "Effectiveness of Annealing of Implanted Layers by Millisecond Laser Pulses," Soviet Physics-Semiconductors, 11(10):1178-1180 (October 1977).

25. Kittel, C. Solid State Physics, Fifth Edition. New York: Wiley and Sons, Inc., 1976.

26. Kressel, H. et al. "Observations Concerning Radiative Efficiency and Deep-Level Luminescence in n-Type GaAs Prepared by Liquid-Phase Epetaxy," Journal of Applied Physics, 39(11):5139-5144 (October 1968).

27. Marcyk, G. T. Glow Discharge Optical Spectroscopy for Measurements of Boron Implanted Distributions in Silicon. Unpublished thesis. Urbana, Illinois: University of Illinois (1973).

28. Mitchell, I. V. et al. "Imvestigation of Te-Doped GaAs Annealing Effects by Optical- and Channeling-Effect Measurements," Journal of Applied Physics, 42(10):3982-3987 (september 1971).

29. Norris, C. B. et al. "Depth-Resolved Cathodoluminescence in Undamaged and Ion-Implanted GaAs, ZnS and CdS," Journal of Applied Physics, 44(7):3209-3221 (July 1973).

30. Pankove, J. I. "Cathodoluminescence of n-Type GaAs," Journal of Applied Physics, 39(12):5368-5372 (November 1968).

31. -----. Electroluminescence. New York: Springer-Verloy, (1977).

32. -----. Optical Processes in Semiconductors. New Jersey: Prentice-Hall, Inc., 1971.

33. Pierce, B. J. Luminescence and Hall Effect of Ion Implanted Layers in ZnO. Unpublished Dissertation, Wright-Patterson AFB, Ohio: Air Force Institute of Technology, (September 1974).

34. ----- and R. L. Hengehold. "Depth-Resolved Cathodoluminescence of Ion-Implanted Layers in Zinc Oxide," Journal of Applied Physics, 47(2):644-651 (February 1976).

35. Sturge, M. D. "Optical Absorption of Gallium Arsenide Between 0.6 and 2.75eV," Physical Review, 127(3):768-773 (August 1, 1962).

36. Wagner, W. R. "Tellurium-Induced Defects in LPE Galluim Arsenide," Institute of Physics Conference, No. 33b, 1977, Chapter 2 (65-73).

37. Willardson, R. K. and A. Beer, editors. Semiconductors and Semimetals. Vol. II, Physics of III-V Compounds. New York: Academic Press, 1966.

38. -----. Semiconductors and Semimetals. Vol. VIII, Transport and Optical Phenomena. New York: Academic Press, 1972.

39. Williams, E. W. "Evidence for Self-Activated Luminescence in GaAs: The Gallium Vacancy-Donor Center," Physical Review, 168(3): 922-928 (April 15, 1968).

40. ----- and D. M. Blacknall. "The Observations of Defects in GaAs Using Photoluminescence at 20°K," Transactions of the Metallurgical Society of AIME, 239:387-394 (March 1967).

41. ----- and H. B. Bebb. "Photoluminescence in Lightly Doped Epitaxial GaAs: Cd and GaAs: Si," Journal of Physics and Chemistry of Solids, 30:1289-1293 (September 1969).

Vita

Ronald Leroy Lusk was born on 29 April 1947 in Walla Walla, Washington, the son of Leroy Elmer and Helen Ruth Lusk. Upon graduating from Walla Walla High School in 1965, he attended Washington State University in Pullman, Washington, from which he graduated with honors with a Bachelor of Science degree in Physics and a commission in the United States Air Force in 1969.

After graduating from flight school at Randolph Air Force Base, San Antonio, Texas, in July 1970, he flew the T-38 as an instructor pilot at Vance AFB, Enid, Oklahoma. After graduating in April 1974 with distinction from the B-52 air crew combat training school at Castle AFB, Atwater, California, he was assigned to the 77th Bombardment Squadron at Ellsworth AFB, South Dakota for three years as a B-52G air crew commander and instructor pilot. During this time, he completed Squadron Officers' School in residence at Maxwell AFB, Montgomery, Alabama, in March 1975. In June 1977, he was assigned to the Air Force Institute of Technology.

<div style="margin-left:3em">

Permanent address: 723 Wallowa Drive
                     Walla Walla, Washington 99362

</div>

REPORT DOCUMENTATION PAGE		READ INSTRUCTIONS BEFORE COMPLETING FORM
1. REPORT NUMBER AFIT/GEP/PH/78D-8	2. GOVT ACCESSION NO.	3. RECIPIENT'S CATALOG NUMBER
4. TITLE (and Subtitle) CATHODOLUMINESCENCE ON THE EFFECTS OF TELLURIUM IMPLANTATION AND LASER ANNEALING IN GALLIUM ARSENIDE		5. TYPE OF REPORT & PERIOD COVERED
		6. PERFORMING ORG. REPORT NUMBER
7. AUTHOR(s) Ronald L. Lusk Captain, USAF		8. CONTRACT OR GRANT NUMBER(s)
9. PERFORMING ORGANIZATION NAME AND ADDRESS Air Force Institute of Technology (AFIT/EN) Wright-Patterson AFB, Ohio 45433		10. PROGRAM ELEMENT, PROJECT, TASK AREA & WORK UNIT NUMBERS Project 2306-R2-13
11. CONTROLLING OFFICE NAME AND ADDRESS Air Force Avionics Laboratory (AFAL-DHR) Wright-Patterson AFB, Ohio 45433		12. REPORT DATE December 1978
		13. NUMBER OF PAGES 63
14. MONITORING AGENCY NAME & ADDRESS(if different from Controlling Office) 6110 2F		15. SECURITY CLASS. (of this report) Unclassified
		15a. DECLASSIFICATION/DOWNGRADING SCHEDULE

16. DISTRIBUTION STATEMENT (of this Report)

Approved for public release; distribution unlimited

17. DISTRIBUTION STATEMENT (of the abstract entered in Block 20, if different from Report)

18. SUPPLEMENTARY NOTES

Approved for public release; IAW AFR 190-17

Joseph F. Hipps, Major, USAF
Director of Information   19 Jan 79

19. KEY WORDS (Continue on reverse side if necessary and identify by block number)

cathodoluminescence   spectra
gallium arsenide   laser
ion-implantation   annealing
luminescence

20. ABSTRACT (Continue on reverse side if necessary and identify by block number)

Six Te implanted GaAs samples were examined by the method of cathodoluminescence to determine the effect of laser annealing. Two of the samples (one 10^{13} fluence and one 10^{14} fluence) were thermally annealed, one sample (10^{13} fluence) was unannealed, and three samples (10^{13} fluence) were laser annealed.

When a laser energy density of 0.07 J/cm^2 was used, it was found that only a small percenrage of the Te ions moved to substitutional sites and the laser radiation created Ga vacancies.

When a laser energy density of 0.06 or 0.8 J/cm^2 was used, the implant

20. layer was damaged by the laser radiation and all luminescence from the implant layer was quenched. Further, the luminescence that was detectable (only at the maximum beam energy of 15KV) was characteristic of the substrate, not the implant layer.